DOI: 10.1534/genetics.104.031344

Dose-Sensitive Autosomal Modifiers Identify Candidate Genes for Tissue Autonomous and Tissue Nonautonomous Regulation by the Drosophila Nuclear Zinc-Finger Protein, Hindsight

Ronit Wilk,*,† Amanda T. Pickup,* Jill K. Hamilton,‡ Bruce H. Reed* and Howard D. Lipshitz*,†,[1]

**Program in Developmental Biology, Research Institute and ‡Division of Endocrinology, The Hospital for Sick Children, Toronto, Ontario M5G 1X8, Canada and †Department of Molecular and Medical Genetics, University of Toronto, Toronto, Ontario M5S 1A8, Canada*

Manuscript received May 18, 2004
Accepted for publication June 7, 2004

ABSTRACT

The nuclear zinc-finger protein encoded by the *hindsight* (*hnt*) locus regulates several cellular processes in Drosophila epithelia, including the Jun N-terminal kinase (JNK) signaling pathway and actin polymerization. Defects in these molecular pathways may underlie the abnormal cellular interactions, loss of epithelial integrity, and apoptosis that occurs in *hnt* mutants, in turn causing failure of morphogenetic processes such as germ band retraction and dorsal closure in the embryo. To define the genetic pathways regulated by *hnt*, 124 deficiencies on the second and third chromosomes and 14 duplications on the second chromosome were assayed for dose-sensitive modification of a temperature-sensitive rough eye phenotype caused by the viable allele, hnt^{peh}; 29 interacting regions were identified. Subsequently, 438 *P*-element-induced lethal mutations mapping to these regions and 12 candidate genes were tested for genetic interaction, leading to identification of 63 dominant modifier loci. A subset of the identified mutants also dominantly modify hnt^{308}-induced embryonic lethality and thus represent general rather than tissue-specific interactors. General interactors include loci encoding transcription factors, actin-binding proteins, signal transduction proteins, and components of the extracellular matrix. Expression of several interactors was assessed in *hnt* mutant tissue. Five genes—*apontic* (*apt*), *Delta* (*Dl*), *decapentaplegic* (*dpp*), *karst* (*kst*), and *puckered* (*puc*)—are regulated tissue autonomously and, thus, may be direct transcriptional targets of HNT. Three of these genes—*apt*, *Dl*, and *dpp*—are also regulated nonautonomously in adjacent non-HNT-expressing tissues. The expression of several additional interactors—*viking* (*vkg*), *Cg25*, and *laminin-α* (*LanA*)—is affected only in a nonautonomous manner.

DURING development, tissues and organs are formed through dynamic cell shape changes and movements that are orchestrated in time and space (reviewed by Gumbiner 1996; Geiger *et al.* 2001). Data gathered from both vertebrate and invertebrate systems have implicated several cell surface, cytoskeletal, and extracellular matrix (ECM) molecules in the establishment and maintenance of cell architecture, cell movement, and tissue integrity during morphogenesis (reviewed by Gumbiner 1996; Lauffenburger and Horwitz 1996; Wilk *et al.* 2004). However, to date, there has been little analysis of genetic regulatory hierarchies that control the expression and function of these molecules in specific tissues.

Previous analyses have shown that the Drosophila *hindsight* (*hnt*) gene encodes a nuclear zinc-finger protein found in several epithelia during development (Yip *et al.* 1997). These include the extraembryonic amnioserosa, the midgut and tracheae of the embryo, and the photoreceptor cells of the developing adult retina (Yip *et al.* 1997; Lamka and Lipshitz 1999; Wilk *et al.* 2000; Reed *et al.* 2001; Pickup *et al.* 2002). HNT expression in these epithelia regulates several local and global morphogenetic processes. For example, the expression of HNT in the amnioserosa is required for embryonic germ band retraction (Yip *et al.* 1997; Lamka and Lipshitz 1999). HNT also plays an important role in embryonic dorsal closure by downregulating JNK signaling in the amnioserosa, thus enabling assembly of the F actin-based purse string in the adjacent, leading edge epidermal cells (Reed *et al.* 2001). During tracheal development, tertiary branching fails (Wilk *et al.* 2000) and, during eye morphogenesis, the shape of individual photoreceptor cells is often abnormal (Pickup *et al.* 2002) in *hnt* mutant tissue. During eye development, HNT function is required for the accumulation of F actin in the apical tip of photoreceptor precursor cells in the ommatidial clusters, as well as in the developing rhabdomere during the pupal period (Pickup *et al.* 2002).

HNT has also been shown to be essential for maintenance of epithelial tissue integrity. While *hnt* mutant tracheae undergo normal specification, invagination,

[1]*Corresponding author:* Program in Developmental Biology, Research Institute, The Hospital for Sick Children, 555 University Ave., Toronto, ON M5G 1X8, Canada. E-mail: lipshitz@sickkids.ca

and primary and secondary branching, at later embryonic stages the epithelial tubes lose their integrity (Wilk *et al.* 2000). Similarly, in *hnt* mutant embryos the amnioserosa falls apart prematurely leading to defects in germ band retraction and dorsal closure (B. H. Reed and H. D. Lipshitz, unpublished observations; see Reed *et al.* 2004). In *hnt* mutant eye tissue, the developing retinal epithelium breaks down at the midpupal stages (Pickup *et al.* 2002).

Thus, *hnt* has all of the hallmarks of a regulatory gene, which functions in specific epithelia to control processes that are required for morphogenesis. However, direct transcriptional targets of HNT as well as genetic pathways that are regulated by HNT remain largely undefined. Here we carry out a series of genetic modifier screens aimed at identifying loci that genetically interact with *hnt*. Two different *hnt* hypomorphic alleles—one a viable eye-specific allele (hnt^{peb}; Pickup *et al.* 2002), the other a leaky embryonic lethal allele (hnt^{308}; Reed *et al.* 2001)—were used to produce sensitized genetic backgrounds in which we could identify dominant modifier loci. Over 60 interactors were identified, including genes encoding transcription factors and cytoskeletal, signal transduction, and ECM components. Expression of a subset of the interactors was assayed in *hnt* mutant tissue. These analyses showed that several genes (*dpp*, *puc*, *kst*, *apt*, and *Dl*) are regulated tissue autonomously by HNT in embryo and/or eye tissue. Expression of three of these (*dpp*, *apt*, and *Dl*) as well as expression of several additional genes (*vkg*, *Cg25C*, and *LanA*) is also affected nonautonomously in *hnt* mutants.

MATERIALS AND METHODS

Drosophila mutants and lines: Most deficiencies, duplications, mutations, *P*-element lethal lines, and enhancer trap lines were obtained from the Bloomington Drosophila Stock Center and are described in FlyBase (http://flybase.bio.indiana.edu/). *In(2LR)lt*$^{616\text{-}L}$*BR29* is a duplication from 60C to 60E (Reed 1992); *Df(1)rb*^{1} has been previously described (Wilk *et al.* 2000). *hnt* mutants included hnt^{XE81} (described in Yip *et al.* 1997), hnt^{1142} (described in Wilk *et al.* 2000), hnt^{308} (described in Reed *et al.* 2001), and hnt^{peb} (described in Yip *et al.* 1997; Pickup *et al.* 2002). $LanA^{3A1}$, $LanA^{4A8}$, vkg^{177}, and $Cgc25C^{234}$ (from N. McGinnis, University of California, San Diego) are described in Gellon *et al.* (1997). To visualize the embryonic tracheal system, the *trachealess* enhancer trap *1-eve-1* was utilized (described in Wilk *et al.* 1996).

Screen for chromosomal regions that dominantly interact with hnt^{peb}: hnt^{peb} virgin females were crossed to males bearing either a deficiency or a duplication *in trans* to a dominantly marked balancer chromosome. Crosses were maintained at 29°, the restrictive temperature at which hnt^{peb} shows a rough eye phenotype (Pickup *et al.* 2002). A total of 124 deficiency lines (*Df*) from the "deficiency kit" for the second and third chromosome were tested, along with 14 duplications (*Dp*) covering most of the second chromosome. hnt^{peb}/*Y*; *Balancer*/+ progeny were compared to the hnt^{peb}/*Y*; *Df* or *Dp*/+ sibs (these sibs were identified by their lack of the dominantly marked balancer). We evaluated and compared the roughness of the eyes between these two groups (~10 pairs of flies). Any consistent difference (enhancement or suppression of the hnt^{peb} rough eye phenotype) was noted and interactors were retested for confirmation.

Screen for loci that dominantly interact with hnt^{peb}: Crosses similar to those described above were also used to identify individual loci that exhibit dominant interactions with hnt^{peb}. The *P*-element lethal lines tested mapped to the regions identified by the first screen and included lines with elements mapping close to, but outside of, the rearrangement breakpoints (this was done to take into account the uncertainties in the cytological breakpoints; Figure 3). In addition to *P*-element lines, a dozen other mutations were tested (see Table 2). Any interaction was confirmed by performing at least two independent crosses. Where possible, additional alleles of the same gene were tested for modification of the rough eye phenotype (see Table 2).

Most of the identified mutations mapped to the second chromosome and behaved as moderate dominant suppressors. One possible explanation for this bias is a difference in genetic background between *P*-element lines on the second compared to the third chromosome. For a subset of the second-chromosome loci, we therefore tested additional alleles induced on distinct genetic backgrounds for interactions with hnt^{peb} (see Table 2). In 64% of the cases (14 of 22) more than one allele interacted with hnt^{peb}. Moreover, hundreds of second-chromosome *P*-element mutations that had been induced on the same genetic background as those exhibiting moderate suppression did not exhibit any dominant genetic interaction with hnt^{peb}. We therefore conclude that most of the interactions are real and that in each case the mutation in the identified modifier gene itself, and not the genetic background, is likely to be responsible for the observed interaction.

Confirmation of genetic interactions utilizing hnt^{308}: Virgin hnt^{308}/*FM7z* females were crossed to balanced mutant males carrying a mutation in the gene to be tested. Embryos from these crosses were collected on grape juice agar plates, aligned in groups of 50 on fresh agar plates, aged for >24 hr at 25° and scored for embryonic lethality. In most cases, the percentage of embryonic lethality was compared to a control cross that was identical except for the absence of the mutation on the autosome (*i.e.*, with the same balancers). Exceptions were *chickadee* (*chic*), *puckered*^{1} (puc^{1}), and *RhoA* (see below). Embryonic lethality was calculated by counting dead (brown eggs with cuticle) and unfertilized eggs (white and undeveloped) and hatched embryos (empty cuticle case). The embryonic lethality was (brown embryos/n), where n was the total number of aligned embryos minus the unfertilized eggs. Embryonic lethality for each mutant was normalized to the lethality observed in control crosses. Most lines were crossed to hnt^{308}/*FM7* female virgins. $chic^{221}$ and $chic^{01320}$ were crossed to hnt^{308}/*FM6* female virgins. The *chic* control was hnt^{308}/*FM6* virgin females crossed to w^{1118}/*Y* males. The control cross for puc^{1} and *RhoA* used hnt^{308}/*FM7* female virgins crossed to Oregon-R males (as described in Reed *et al.* 2001). Embryonic lethality among specific controls was as follows: *CyO*, 0.125 ± 0.08; *TM3*, 0.161 ± 0.05; *TM1*, 0.122; *TM6B*, 0.146; and *chic* control, 0.08. The following embryonic lethalities, normalized to control values of 1.0, were calculated and used to create Figure 4: (*viking*) vkg^{01209}/*CyO*, 0.575; vkg^{177}/*CyO*, 0.95; vkg^{k16721}/*CyO*, 0.16; vkg^{k00236}/*CyO*, 0.17; vkg^{k07138}/*CyO*, 0.17; vkg^{k16502}/*CyO*, 0.13; $Cg25C^{k00405}$/*CyO*, 0.93; $Cg25C^{234\text{-}9}$/*CyO*, 0.067; (*Laminin A*) $LanA^{3A1}$/*TM1 Me*, 0.088; $LanA^{4A8}$/*TM1 Me*, 0.088; (*karst*) kst^{01318}/*TM3 Sb*, 0.22; kst^{1}/*TM6B*, 0.17; kst^{2}/*TM6B*, 0.15; (*turtle*) $tutl^{k14703}$/*CyO*, 0.086; (*thickveins*) tkv^{k16713}/*CyO*, 0.09; (*heixuedian*) $heix^{k11403}$/*CyO*, 0.1; (*Delta*) Dl^{05151}/*TM3 Sb*, 0.067; (*slow border cells*) $slbo^{ry8}$/*CyO*, 0.11; $puc^{A251.1f3}$/*TM3 Sb*, 0.148; *Df(3L)kto2/TM6B,Tb*^{1}, 0.038; $chic^{221}$/*CyO*, 0.11; and $chic^{01320}$/*CyO*, 0.104.

The statistical significance of the results was determined using the χ^2 test (Dixon and Massey 1957). To calculate the χ^2, we used the results from the balancer control crosses to

generate the expected frequencies and the results from the testcrosses with candidate mutations to generate the observed frequencies. We considered a *P*-value of <0.05 to be significant. If the percentage of embryonic lethality increased or decreased significantly when the mutation was present, the mutation is listed as a dominant enhancer or a suppressor of hnt^{308} embryonic lethality, respectively.

Test for molecular regulation by HNT: Embryos from the following candidate enhancer trap lines were stained with anti-β-galactosidase antibody: $Dl^{05151}/TM3$, $chic^{K13321}/Cyo$, $chic^{35A}/Cyo$, $chic^{13E}/Cyo$, $chic^{RM1}/Cyo$, $chic^{11}/Cyo$, $kst^{01318}/TM3$, vri^{K05901}/CyO, $puc^{A251.1F3}/TM3$, dpp^{10638}/CyO, apt^{K15608}/CyO, apt^{03041}/CyO, and $RhoA^{K02107b}/CyO$. If expression was detected in either the tracheal system or the amnioserosa, expression was assayed in *hnt* mutants as follows. Virgin $hnt^{XE81}/FM7z$ females were crossed to males from the following enhancer trap lines: $Dl^{05151}/TM3$, $puc^{A251.1F3}/TM3$, dpp^{10638}/CyO, tkv^{K16713}/CyO, apt^{03041}/CyO, and $Rho1^{K02107b}/CyO$. Overnight embryo collections from these crosses were immunostained for β-galactosidase to determine if there was any difference in staining between hnt^{XE81} mutant embryos with the enhancer trap and their wild-type sibs that only carried the enhancer trap (the *ftz-lacZ* marker on the FM7z balancer chromosome distinguished them from the *hnt* embryos).

Standard protocols were used to generate FLP-induced *hnt* clones in the eye disc (Xu and Rubin 1993). The FRT line w^{1118} $P\{w^{+mC}=piM\}5A$ $P\{w^{+mC}=piM\}10D$ $P\{ry^{+t7.2}=neoFRT\}18A$ and the FLP recombinase stock w^{1118}; *MKRS*, $P\{ry^{+t7.2}=hs\text{-}FLP\}86E/TM6B$ Tb^{1} were obtained from the Bloomington Drosophila Stock Center. Eye discs were dissected from third instar larvae of the genotype 182piM $FRT/hnt^{XE81}FRT{:}Dl^{05151}/FLP$, 182piM $FRT/hnt^{XE81}FRT{:}$ kst^{01318}/FLP, or 182piM FRT/hnt^{EH704a} $FRT{:}FLP/+$ and immunostained with α-HNT (to identify *hnt* patches) and either α-β-galactosidase (for *Dl-lacZ* and *kst-lacZ*) or α-Apontic antibody, respectively, to determine whether the *hnt* mutant area shows any difference in staining for the candidate gene product.

Immunostaining and microscopy: Staining was carried out using standard procedures with the following antibodies: mouse monoclonal anti-Drosophila collagen type IV (from L. I. Fessler, University of California, Los Angeles; 1:70 dilution); rabbit anti-Drosophila laminin [from L. I. Fessler; used at 1:700 dilution as described in Fessler *et al.* (1987)]; rabbit anti-β-galactosidase (Cappel, Malvern, PA; 1:1000 dilution); chicken anti-β-galactosidase (ab-cam; 1:1000 dilution); guinea pig anti-tracheal lumen 55 [from B. Shilo; used at 1:150 dilution as described in Reichman-Fried *et al.* (1994)]; rabbit anti-Apontic/Tracheae defective [APT; from R. Schuh, Max Planck Institute; used at 1:30 dilution as in Eulenberg and Schuh (1997)]; mouse monoclonal anti-HNT, used at 1:20 dilution as described in Yip *et al.* (1997). Double staining for laminin and tracheal lumen as well as double staining for TDF and HNT was performed as previously described (Wilk *et al.* 2000). HRP-secondary antibodies were used for light microscopy (Jackson, West Grove, PA; 1:300 dilution); rhodamine and FITC-conjugated secondary antibodies were used for confocal analyses (Jackson; 1:300 dilution).

Light microscopy was carried out using a Zeiss Axioplan 2 imaging microscope. Images were captured with a Spot digital camera (Diagnostic Instruments) and Spot software or with a Zeiss AxioCam digital camera and AxioVision 3.1 software. Confocal analyses were conducted using a Zeiss inverted microscope with LSM 510 software. Images were processed with PhotoShop (Adobe) and Illustrator software (Adobe).

RESULTS

Identification of autosomal regions that exhibit dominant genetic interactions with hnt^{peb}: To identify chromosomal regions that genetically interact with *hnt*, we performed a genetic screen for dose-dependent modifiers of the temperature-sensitive rough eye phenotype exhibited by the viable allele, hnt^{peb} (Figure 1; Yip *et al.* 1997; Pickup *et al.* 2002). We tested 58 deficiencies on the second chromosome and 64 on the third chromosome that, respectively, remove a total of ~84% and ~78% of the loci on these chromosomes (Figure 2). In addition we used 14 duplications that cover ~84% of the second chromosome (Figure 2). hnt^{peb} males carrying one copy of the deficiency or the duplication were compared to sibling hnt^{peb} males carrying a balancer chromosome (for details, see materials and methods). Dominant genetic modifiers of hnt^{peb} were identified on the basis of a consistent and reproducible alteration in eye roughness. Twenty-nine deficiencies or duplications consistently modified the hnt^{peb} rough eye phenotype (~21% of the lines tested; see example in Figure 1C): 17 were suppressors and 12 were enhancers, representing 19 different regions (8 on the second and 11 on the third chromosome; see Figures 2 and 3; Table 1).

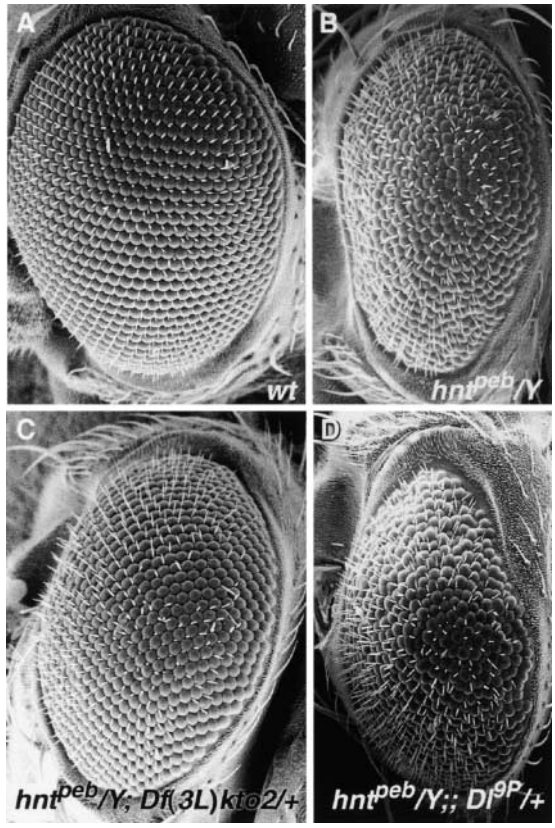

Figure 1.—Dose-dependent modification of the hnt^{peb} rough eye phenotype is shown in scanning electron micrographs of adult eyes. (A) Eye from a wild-type male fly. (B) Eye from an hnt^{peb} male fly raised at the restrictive temperature, showing a rough eye due to disorganization of facets (modified from Pickup *et al.* 2002). (C) Eye from an hnt^{peb}/Y; $Df(3L)kto2/+$ fly raised at the restrictive temperature showing suppression of the hnt^{peb}/Y eye phenotype. (D) Eye from hnt^{peb}/Y; $Dl^{9P}/+$ fly raised at the restrictive temperature showing enhancement of the hnt^{peb}/Y eye phenotype.

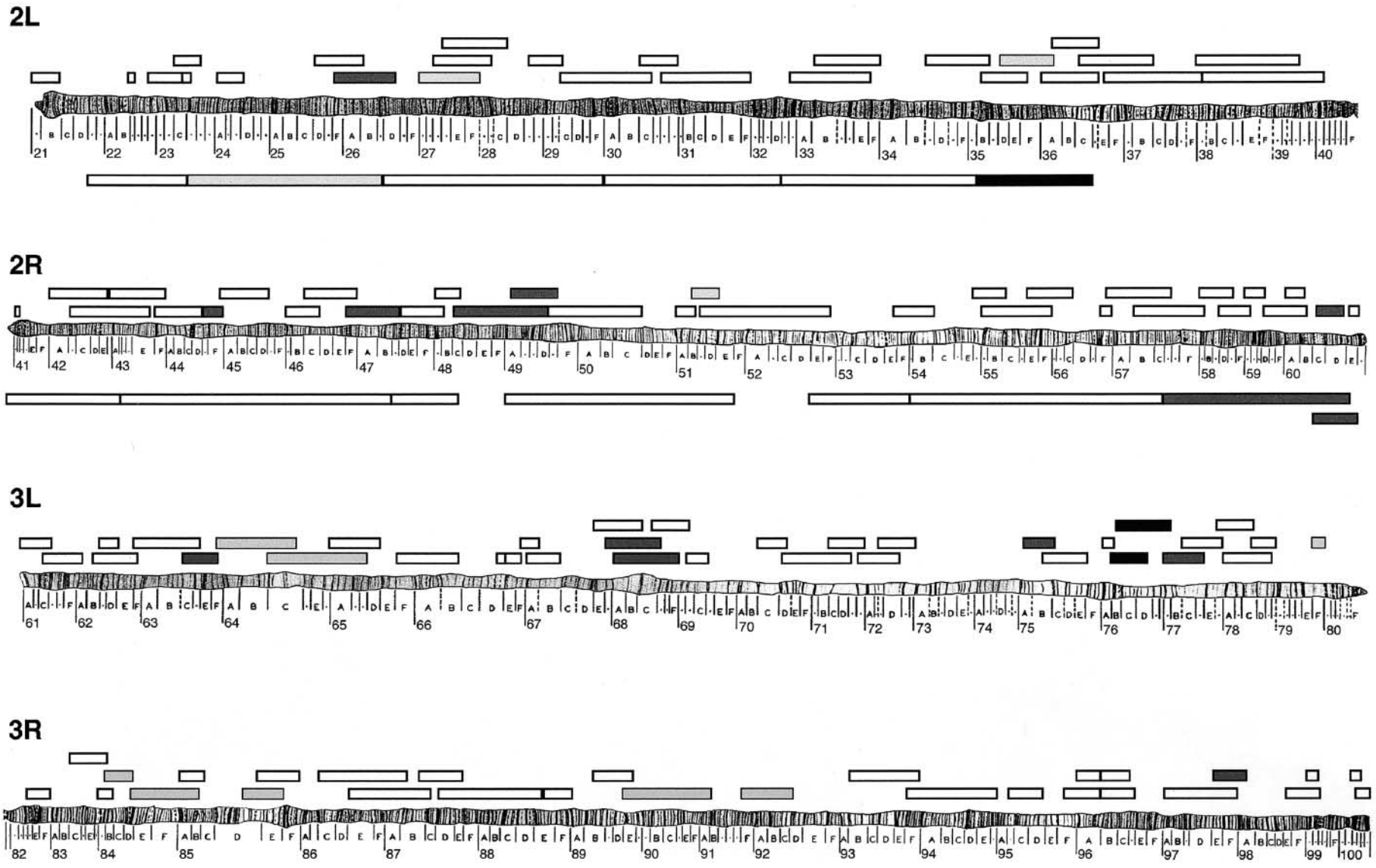

FIGURE 2.—Dose-dependent modification of *hnt*^{peb} by autosomal deficiencies and duplications. The schematic represents all the regions in the fly chromosome that were found to genetically modify the mild rough eye phenotype exhibited by *hnt*^{peb} at 29°. Each box above the chromosomes represents the region that is missing in a particular fly line (deficiency). The boxes below the chromosomes represent the region that is duplicated in a certain fly line (duplication). The results from the genetic interactions are grayscale coded: white, no interaction; dark gray, moderate suppressor; black, suppressor; and light gray, enhancer. A list of the interacting regions can be found in Table 1.

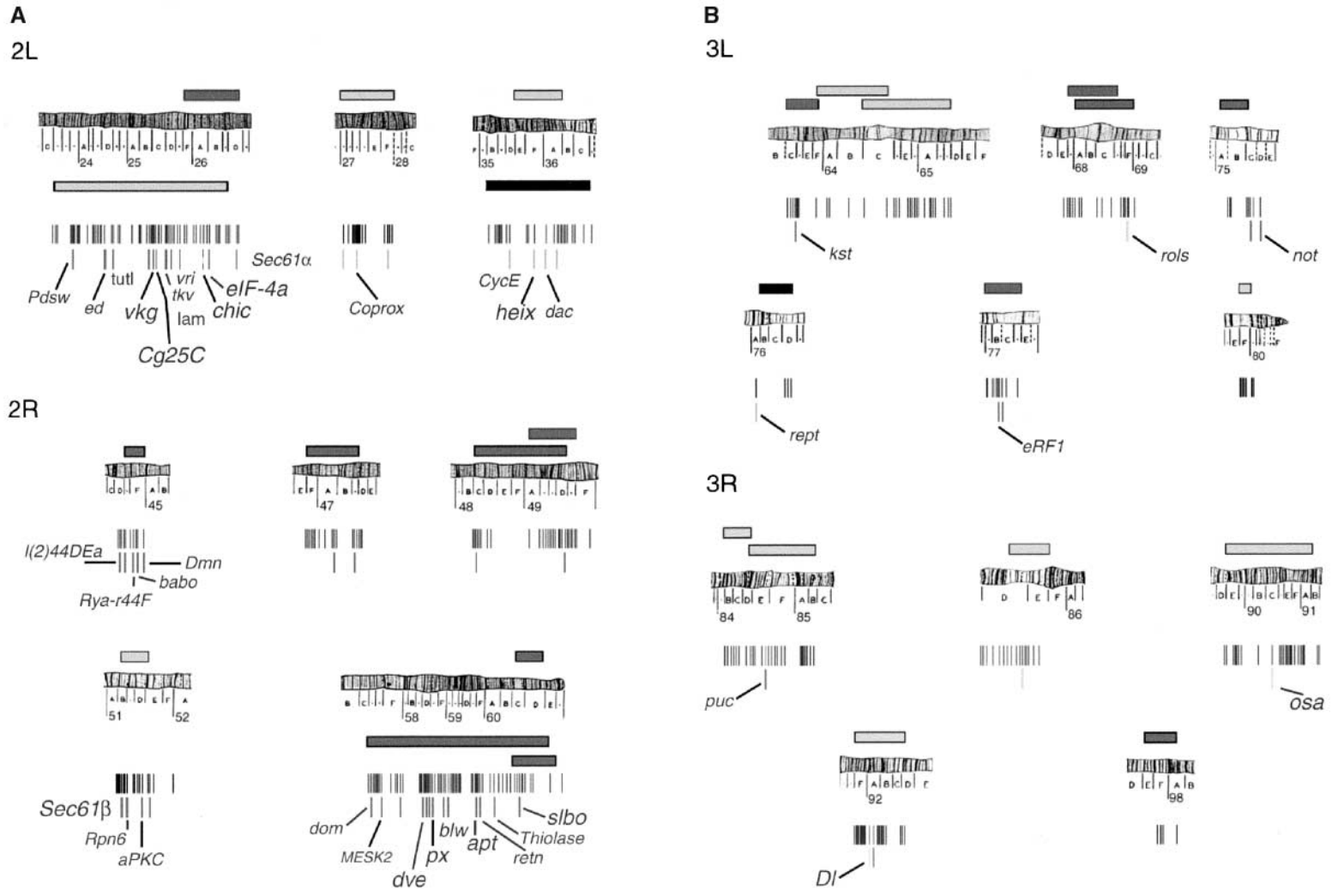

FIGURE 3.—Schematic of *P*-element lines that genetically interact with hnt^{peb}. (A) Chromosome 2. (B) Chromosome 3. All the *P*-element lethal stocks that mapped to any of the interacting regions defined by deficiencies or duplications were tested for modification of the hnt^{peb} rough eye phenotype. A vertical line marks each fly line that was tested. A grayscale vertical line underneath represents any modification to the hnt^{peb} rough eye phenotype. The grayscale code and the schematic representation of deficiencies and duplications are the same as in Figure 2. The name of the gene mutated by an interacting *P* element is shown. Larger font represents genes where at least two alleles genetically interact with hnt^{peb}. Details are given in Table 2.

TABLE 1

Regions of the second and third chromosomes that genetically interact with *hnt^{peb}*

Stock	Deficiency (Df) or duplication (Dp)	Cytology
	Suppressor	
Dp(2;2)Cam6 (4518)	Dp	35B;36C
Df(3L)kto2 (3617)	Df	76B1–2;76D5
Df(3L)XS533 (5126)	Df	76B4;77B
	Moderate suppressor	
Df(2L)E110 (490)	Df	25F3–26A1;26D3–11
Df(2R)H3E1 (201)	Df	44D1–4;44F12
Df(2R)stan2 (596)	Df	46F1–2;47D1–2
Df(2R)vg135 (1642)	Df	48C–48D;49D
Df(2R)vg-C (754)	Df	49A4–13;49E7–F1
Dp(2;2)Cam16 (2622)	Dp	57C4–6;60E4
In(2LR)lt$^{616\text{-}L\ BR27\text{-}R}$	Dp	60C;60E
Df(2R)Px2 (2604)	Df	60C5–6;60D9–10
Df(3L)HR119 (3649)	Df	63C2;63F7
Df(3L)vin2 (2547)	Df	67F2–3;68D6
Df(3L)vin5 (2611)	Df	68A2–3;69A1–3
Df(3L)W10 (2608)	Df	75A6–7;75C1–2
Df(3L)rdgC-co2 (2052)	Df	77A1;77D1
Df(3R)D605 (823)	Df	97E3;98A5
	Enhancer	
Df(3R)Dl-BX12 (3012)	Df	91F1–2;92D3–6
	Moderate enhancer	
Dp(2;2)Cam2 (3394)	Dp	23D1–2;26C1–2
Df(2L)Dwee-delta5 (3571)	Df	27A;28A
Df(2L)r10 (1491)	Df	35D;36A6–7
Df(2R)knSA3 (1150)	Df	51B5–11;51D7–E2
Df(3L)GN24 (3686)	Df	63F6–7;64C13–15
Df(3L)ZN47 (3096)	Df	64C;65C
Df(3L)Delta1AK (4370)	Df	79E5–F1;79F2–6
Df(3R)Antp17 (1842)	Df	84B1–2;84D11–12
Df(3R)p712 (1968)	Df	84D4–6;85B6
Df(3R)by10 (1931)	Df	85D8–12;85E7–F1
Df(3R)DG2 (4431)	Df	89E1–F4;91B1–B2

Dose-dependent modifiers of the mild rough eye phenotype observed in *hnt^{peb}* adult fly eyes. The stock name is followed by the Bloomington stock number in parentheses. Each line represents either a deficiency (Df) or a duplication (Dp) that enhances or suppresses the *hnt^{peb}* rough eye phenotype. The region of the chromosome that is either duplicated or absent is listed in the cytology column.

Mutations in 63 autosomal loci dominantly interact with *hnt^{peb}*: To identify interacting genes in the autosomal regions defined by the deficiencies and duplications, 438 individual *P*-element lethal lines mapping to the 19 identified regions were tested for their ability to dominantly modify the *hnt^{peb}* rough eye phenotype (for details, see MATERIALS AND METHODS; Figure 3). Whenever possible, the interactions were confirmed with additional alleles of each putative modifier gene (Table 2; Figure 1D). In addition, we tested mutations in 12 candidate genes, including members of the JNK pathway (*anterior open* and *jun-related antigen*) and the small GTPase, *RhoA* (see Table 2).

In total, 470 crosses were performed and 89 interacting mutant lines were identified (Figure 3; Table 2): 77 dominantly suppress and 12 dominantly enhance the *hnt^{peb}* rough eye phenotype. These represent 63 different loci: 45 with genetically and/or molecularly characterized gene products and 18 with novel or uncharacterized products. The interacting genes can be grouped into several different functional classes on the basis of the cellular and molecular functions of their encoded proteins (Table 2): components of the cytoskeleton (*e.g.*, profilin and β_{Heavy}-spectrin), the extracellular matrix (*e.g.*, collagen type IV, α1 and α2 chains), signal transduction pathways (*e.g.*, Delta and Puckered), nu-

TABLE 2

Loci that genetically interact with *hnt^{peb}*

Locus (cytology)	Allele	Genetic interaction (expected direction)	Molecular identity of gene product
		Components of the cytoskeleton	
chickadee (*chic*) (26A9–B1)	*11*	Su (+)	Profilin; actin polymerization/depolymerization
	01320	Su (+)	
	221	Su (+)	
	k13321	E (−)	
cactus[a] (35F9–11)	*4*	Su (−)	Transcription factor; cytoplasmic sequestration of Dorsal
	1	No interaction	
Dynamitin (*Dmn*) (44F6–8)	*k16109*	Su (+)	Dynactin motor; microtubule-based movement
RhoA[a] (52E4)	*J3.8*	Su (NR)	Rho small monomeric GTPase
	E3.10	No interaction	
karst (*kst*) (63C5–D1)	*01318*	Su (+)	β_{Heavy}-spectrin; actin binding, microtubule binding
rolling pebbles (*rols*) (68F1)	*08232*	E (−)	Component of the cytoplasm; involved in myoblast fusion
		Extracellular matrix component	
viking (*vkg*) (25C1)	*01209*	Su (+)	Type IV collagen α2 chain
	k00236	Su (+)	
	k07138	Su (+)	
	k16721	Su (+)	
	k16502	Su (+)	
	177-27	Su (+)	
Cg25C (25C1–2)	*k00405*	Su (+)	Type IV collagen α1 chain
	234-9	Su (+)	
		Components of signal transduction pathways	
		EGFR signaling pathway	
echinoid (*ed*) (24D2–4)	*k01102*	Su (+)	Contains immunoglobulin domains
MESK2 (57E6–9)	*k0019*	Su (−)	Suppressor of KSR2; alpha/beta-hydrolase domains
EgfR[a] (57E9–F1)	*f1*	E (+)	Epidermal growth factor receptor; protein tyrosine kinase
		TGFβ/Dpp signaling pathway	
thickveins (*tkv*) (25C9–D1)	*k16713*	Su (+)	Protein kinase; involved in dorsal closure and tracheal system development
	09415	No interaction	
baboon (*babo*) (44F12–45A1)	*k16912*	Su (+)	Type I TGFβ receptor; serine/threonine kinase
	32	No interaction	
		JNK signaling pathway	
anterior open[a] (*aop*) (22D1)	*1*	Su (NR)	RNA polymerase II transcription factor; transcriptional repressor
Jun related antigen (*Jra*)[a] (46E4–5)	*1*	Su (+)	Transcription factor bZIP; Jun related
puckered (*puc*) (84E10–13)	*A251.1f3*	Su (−)	Protein tyrosine phosphatase; Jun kinase (JNK) phosphatase
		Notch signaling pathway	
l(2)44DEa (44D3–6)	*k10313*	Su (+)	Acetate-CoA ligase; interacts with *l(1)Sc* and *N*
	05847	Su (+)	

(*continued*)

TABLE 2

(Continued)

Locus (cytology)	Allele	Genetic interaction (expected direction)	Molecular identity of gene product
Delta (Dl) (92A1–2)	*05151*	E (+)	Notch receptor ligand
	X	E (+)	
	9P	E (+)	
		Other signaling pathways	
plexus (*px*) (58E3–8)	*k08316*	Su (−)	Localized to the nucleoplasm; interacts genetically with *Delta*, *rho*, and *EGFR*
	k08134	Su (−)	
Atypical protein kinase C (*aPKC*) (51D7–8)	*k06403*	Su (−)	Atypical protein kinase C; mutants affect epithelial apical-basal polarity; associates with Bazooka; expressed apically in tracheae and other epithelia, not in amnioserosa
		Nucleic acid binding	
vrille (*vri*) (25D4–5)	*k05901*	Su (+)	Transcription factor; bZIP; expressed in amnioserosa, tracheae, eye, and other tissues
eIF-4a (26B1–2)	*02439*	Su (+)	RNA helicase; translation initiation factor; expressed ubiquitously in embryos
	k14518	Su (+)	
	k01501	No interaction	
dachshund (*dac*) (36A2)	*P*	Su (−)	Transcription factor; expressed in CNS and eye disc
domino (*dom*) (57D4–8)	*k08108*	Su (−)	Transcription factor; helicase; involved in cell proliferation; expressed in hemocytes and other tissues
defective proventriculus (*dve*) (58D1–2)	*01738*	Su (−)	Transcription factor; homeodomain
	k06515	Su (−)	
apontic (*apt*) (59F1–2)	*k15608*	Su (−)	Transcription factor; expressed in amnioserosa, tracheal system, and other tissues; mutations affect the larval tracheal system and the embryonic heart
	09049	Su (−)	
	03041	Su (−)	
	06369	Su (−)	
retained (*retn*) (59F2–3)	*02535*	Su (−)	DNA-binding protein; expressed in the amnioserosa and the brain
slow border cells (*slbo*)	*ry7*	S (+)	Transcription factor; bZIP; required for border cell migration; expressed in border follicle cells, embryonic foregut, midgut, and epidermis
	ry8	Su (+)	
	01310	Su (+)	
reptin (*rept*) (76A3–4)	*06945*	Su (+)	DNA binding; helicase
osa (90C1–2)	*00090*	E (+)	DNA binding; expressed in the eye disc morphogenetic furrow
	Avr1	E (+)	
glass[a] (91A3)	*1*	E (+)	C_2H_2 zinc-finger transcription factor; eye photoreceptor development
	2	E (+)	
	3	No interaction	

(*continued*)

TABLE 2

(Continued)

Locus (cytology)	Allele	Genetic interaction (expected direction)	Molecular identity of gene product
		Localized to cell membranes	
turtle (*tutl*) (24E1–4)	*k14703*	Su (+)	Contains immunoglobulin domains; flight behavior
	01081	No interaction	
lamin (*lam*) (25E6–F1)	*k11511*	Su (+)	Nuclear membrane protein; involved in nuclear envelope reassembly; mutations affect cytoplasmic extensions for terminal cells of the tracheal system
	04643	No interaction	
heixuedian (*heix*) (35F7–8)	*k11403*	Su (−)	Plasma membrane component; integral membrane protein
	1	Su (−)	
Rya-r44F (44F3–8)	*k04913*	Su (+)	Ryanodine receptor; caffeine-sensitive calcium release channel; localized to the ER membrane
		Miscellaneous	
Pdsw (23F3)	*k10101*	Su (+)	NADH dehydrogenase
*Sec61*α (26D7–8)	*k04917*	Su (+)	Protein transporter
Coprox (27C6–8)	*k10617*	Su (−)	Coproporphyrinogen oxidase
Cyclin E (*CycE*) (35D4)	*05206*	Su (−)	G_1/S specific cyclin
	k05007	No interaction	
*Sec61*β (51B6)	*k03307*	Su (−)	Protein transporter; component of the translocon
	07214	Su (−)	
Proteasome p44.5 subunit (*Rpn6*) (51C1)	*k00103*	Su (−)	Involved in proteolysis; component of the proteasome regulatory particle
bellwether (*blw*) (59B2)	*k00212*	Su (−)	Hydrogen transporting ATP synthase
	03972	Su (−)	
	1	No interaction	
Thiolase (60A5–7)	*k09828*	Su (−)	Acetyl CoA acyltransferase
	00628	No interaction	
non-stop (*not*) (75D4)	*02069*	Su (NR)	Ubiquitin protease; axonal target recognition
eRF1 (77B4–5)	*neo28*	Su (+)	Translation release factor involved in termination of protein synthesis
		Unknown or novel	
l(2)k10001 (25B8–9)	*k10001*	Su (+)	Unknown
l(2)k00605 (27A1–2)	*k00605*	Su (−)	Unknown
l(2)k10113 (27F4–6)	*k10113*	Su (−)	Unknown
l(2)k13905 (36A10–11)	*k13905*	Su (−)	Unknown
l(2)s1878 (44D5–6)	*s1878*	Su (+)	Unknown
l(2)00297 (47A13–14)	*00297*	Su (+)	Unknown
l(2)k15826 (47C3–4)	*k15826*	Su (+)	Unknown; homology to a transtyretin-like protein (BLAST)

(*continued*)

TABLE 2

(Continued)

Locus (cytology)	Allele	Genetic interaction (expected direction)	Molecular identity of gene product
fs(2)neo12 (48C)	*1*	Su (+)	Unknown
unchained (49D1–50D1)	*k15501*	Su (+)	Novel; mutations affect the chordotonal organ
charlatan (51E2)	*02064*	Su (−)	Novel; transcription factor domains; mutations affect the chordotonal organ and the PNS
	k04218	No interaction	
l(2)03605 (57F8–10)	*03605*	Su (−)	Unknown
l(2)k13211 (58D6–7)	*k13211*	Su (−)	Unknown
l(2)k06617 (58D6–7)	*k06617*	Su (−)	Unknown
l(2)k00611 (58F4–5)	*k00611*	Su (−)	Unknown; transcription factor domains
l(3)L3930 (75C5–6)	*L3930*	Su (+)	Unknown
ms(3)neo94 (77B–C)	*1*	Su (+)	Unknown
l(3)10615 (85D16)	*10615*	E (+)	Unknown
l(3)neo51 (92A)	*1*	Su (−)	Unknown

All loci are listed that modify the rough eye phenotype exhibited by hnt^{peb} at 29°, including all the *P*-element lines and other types of mutations. The table is organized by "functional classes." Su, suppressor; E, enhancer; NR, not relevant (the gene does not map to an interacting region). Plus indicates that the corresponding deficiency showed the same result; minus indicates that it did not show the same result.

[a] Additional, candidate gene not within an interacting region defined in Table 1.

cleic acid binding proteins (*e.g.*, Slow border cells and Apontic), proteins localized to cell membranes (*e.g.*, lamin), and miscellaneous and novel genes (Table 2).

Most of the identified loci are general rather than stage- or tissue-specific dominant modifiers of *hnt*: HNT is expressed in several different tissues during development, including the extra-embryonic amnioserosa, the tracheal system, and the larval eye imaginal disc (Yip *et al.* 1997). It has specific roles in each of these tissues as well as general roles in all tissues in which it is expressed (Lamka and Lipshitz 1999; Wilk *et al.* 2000; Reed *et al.* 2001; Pickup *et al.* 2002). Since our primary screen was performed utilizing the severity of the eye phenotype as readout, we wanted to distinguish between eye-specific and more general genetic interactions.

hnt^{308} is a *P*-element insertion in the 5′ regulatory region of the *hnt* gene and causes embryonic lethality with some larval, pupal, and adult escapers (Reed *et al.* 2001). We therefore retested hnt^{peb}-interacting mutations in 11 loci for modification of hnt^{308} by assaying for dominant enhancement or suppression of embryonic lethality (see materials and methods). The genes retested encode transcription factors (*apt* and *slbo*), cytoskeletal regulatory proteins (*RhoA*, *kst*, and *chic*), members of signal transduction pathways (*tkv*, *Dl*, and *puc*), membrane-associated proteins (*turtle* and *heixuedian*), and components of the extracellular matrix (*vkg* and *Cg25C*). Since both laminin and collagen IV are major components of the extracellular matrix, we also tested mutations in a candidate gene, *LanA*, not identified in the initial screen; *LanA* encodes Drosophila laminin-α. As a control for genetic interactions with different *hnt* alleles we also tested a deficiency, *Df(3L)kto2*, which had been identified in our screen as a strong suppressor of the hnt^{peb} rough eye phenotype (Figure 1C; Table 1).

For most genes tested (7 of 10) at least 1 allele exhibits a significant dominant genetic interaction with both hnt^{peb} and hnt^{308} (Figure 4; Table 3). Considering all alleles tested, 70% show an interaction with both *hnt* alleles (12 of 17; Table 3). Of these, half of the interactions (6 of 12) are in the same direction (*i.e.*, suppressor or enhancer of both hnt^{peb} and hnt^{308}). *Df(3L)kto2* dominantly suppresses both hnt^{peb} and hnt^{308} (Figure 4; Table 3), suggesting that an unknown *hnt*-interacting gene maps within this deficiency (*reptin*, which maps distal to the deficiency breakpoint, weakly suppresses and therefore cannot explain the strong interaction seen with the deficiency). In addition, two different alleles of *LanA* interact with hnt^{308} (Figure 4; Table 3). Of the genes tested only three—*heix* (1 allele), *puc* (2 alleles), and

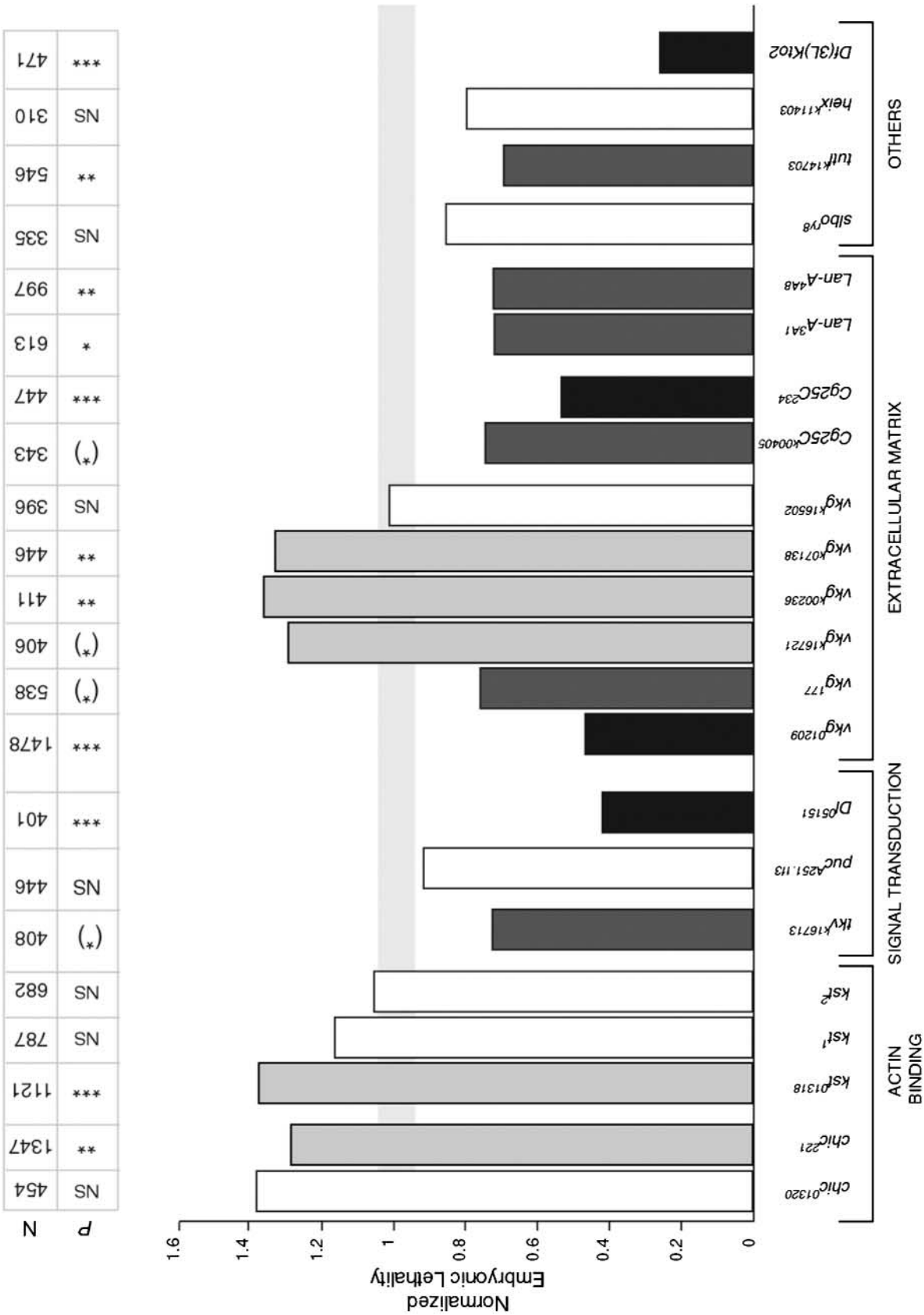

FIGURE 4.—Genetic interactions with *hnt*^{308}. Fly lines that were crossed to *hnt*^{308} virgin females are shown, organized by their biological function. Embryonic lethality was scored for the progeny of all crosses. The data are normalized to the appropriate control, and controls are all normalized to one. The light gray horizontal bar represents the normalized control plus or minus the normalized error bars. The number of embryos scored (N) and the P-values for the χ^2 test are shown. Statistically significant interactions are shaded as in Figures 2 and 3. NS, no significant interaction; (*), $P = 0.05$–0.1; *, $P = 0.025$–0.05; **, $P = 0.01$–0.025; ***, $P \ll 0.005$.

TABLE 3

Genetic interactions with *hnt*^{308}

Gene	Allele	Genetic interactions with *hnt*^{peb}	Genetic interactions with *hnt*^{308}	*P*	*N*	AS	TR	Eye
chickadee	*01320*	Su	NS (1.23)	0.1–0.5	454	+	+	+
	221	Su	E (1.38)	0.01–0.025**	1347	+	+	+
RhoA	*J3.8*	Su	Su (ND)	—[a]	1195	+	+	+
	k07236	ND	NS (ND)	—[a]	810	+	+	+
karst	*01318*	Su	E (1.37)	≪0.005***	1121	ND	+ (apical)	+
	1	ND	NS (1.65)	0.1-0.5	787	ND	+ (apical)	+
	2	ND	NS (1.05)	0.5-0.9	682	ND	+ (apical)	+
viking	*01209*	Su	Su (0.46)	≪0.005***	1478	−	+ (basal lamina)[b]	+ (peripodial epithelium)[b]
	177	Su	Su (0.75)	0.05–0.1(*)	538	−	+ (basal lamina)[b]	+ (peripodial epithelium)[b]
	k16721	Su	E (1.28)	0.05–0.1(*)	406	−	+ (basal lamina)[b]	+ (peripodial epithelium)[b]
	k00236	Su	E (1.36)	0.01–0.025 **	411	−	+ (basal lamina)[b]	+ (peripodial epithelium)[b]
	k07138	Su	E (1.33)	0.01–0.025 **	446	−	+ (basal lamina)[b]	+ (peripodial epithelium)[b]
	k16502	Su	NS (1.01)	0.5–0.9	396	−	+ (basal lamina)[b]	+ (peripodial epithelium)[b]
Cg25C	*k00405*	Su	Su (0.75)	0.05–0.1(*)	343	−	+ (basal lamina)[b]	+ (peripodial epithelium)[b]
	234-9	Su	Su (0.54)	<0.005***	447	−	+ (basal lamina)[b]	+ (peripodial epithelium)[b]
LanA	*3A1*	ND	Su (0.72)	0.025–0.05*	613	ND	+ (basal lamina)[b]	+
	4A8	ND	Su (0.72)	0.01–0.025**	997	ND	+ (basal lamina)[b]	+
thickveins	*k16713*	Su	Su (0.72)	0.05–0.1(*)	408	ND	+	+
puckered	*A251.1f3*	Su	NS (0.92)	0.5–0.9	446	+	ND	+
	1	ND	NS (ND)	—[a]	610	+	ND	+
Delta	*05151*	E	Su (0.48)	≪0.005***	401	+[b]	+	+
slow border cells	*ry8*	Su	NS (0.85)	0.1–0.5	335	ND	+	ND
turtle	*k14703*	Su	Su (0.69)	0.01–0.025**	546	ND	ND	ND
heixuedian	*k11403*	Su	NS (0.8)	0.1–0.5	310	ND	ND	ND
Df(3L)kto2	NA	Su	Su (0.26)	≪0.005***	471	NA	NA	NA

Comparisons are shown between genetic interactions with *hnt*^{308} *vs.* the ones observed with *hnt*^{peb}. E denotes enhancement and Su denotes suppression of *hnt*^{308} embryonic lethality (EL; see MATERIALS AND METHODS). The normalized EL is shown in parentheses. The last three columns show whether (+) or not (−) the gene is expressed in the amnioserosa (AS), embryonic tracheal system (TR), or the developing eye (Eye). NS, no significant interaction; ND, not determined; NA, not applicable; *P*, the *P*-value for the χ^2 test; *N*, number of embryos assayed. Asterisks are as in Figure 4.

[a] Method of analysis was as in REED *et al.* (2001) and differed slightly from that used in this study; thus, *P*-values were not calculated.

[b] Expression was determined in this study.

slbo (1 allele)—failed to show significant interactions with *hnt*^{308}. We conclude that the majority of genes tested in both the adult and the embryo define general rather than stage- or tissue-specific dominant modifiers of *hnt*. Detailed results for a subset of the *hnt*-interacting genes are presented below.

Mutations in genes encoding proteins with a role in F actin cytoskeletal organization dominantly interact with *hnt*: Three of the *hnt*-interacting loci encode proteins that have a role in the assembly or function of the F actin-based cytoskeleton: *chic*, *kst*, and *RhoA*. These were of particular interest in light of the previously reported defects in the actin-based cytoskeleton in *hnt* mutants (REED *et al.* 2001; PICKUP *et al.* 2002). *kst* encodes Drosophila β_{Heavy}-spectrin, which has actin crosslinking activity and associates with the plasma membrane (THOMAS and KIEHART 1994). *chic* encodes profilin, a central player in the regulation of actin polymerization (COOLEY

et al. 1992; Verheyen and Cooley 1994). Small GTPases such as RhoA (also called Rho1) function in organization of the actin cytoskeleton as well as adherens junction formation, intracellular targeting of proteins, phosphorylation of catenins, and regulation of cell signaling pathways (reviewed by Tepass *et al.* 2001; Van Aelst and Symons 2002; Wilk *et al.* 2004).

Four alleles at the *chic* locus—$chic^{11}$, $chic^{01320}$, $chic^{221}$, and $chic^{k13321}$—interact genetically with hnt^{peb}; three suppress and one enhances the rough eye phenotype (Table 2). Two alleles were tested for interaction with hnt^{308}: one, $chic^{01320}$, enhances the embryonic lethality but not at a statistically significant level, while the other, $chic^{221}$, significantly enhances the lethality (Figure 4; Table 3). The direction of the $chic^{01320}$ interaction differs in the eye (suppressor) *vs.* the embryo (enhancer). One allele of *kst*, kst^{01318}, suppresses the rough eye phenotype of hnt^{peb} (Table 2) while it enhances the embryonic lethality of hnt^{308} (Table 3; Figure 4); two additional alleles, kst^{1} and kst^{2}, show slight—but not statistically significant—enhancement of the embryonic lethality (Table 3; Figure 4). The recessive lethal allele $RhoA^{J3.8}$ suppresses the hnt^{peb} and the hnt^{308} phenotypes, while the milder, nonlethal allele $RhoA^{K07236}$ does not interact with hnt^{308} (Tables 2 and 3).

We conclude that *kst*, *chic*, and *RhoA* are general rather than tissue- or stage-specific dominant modifiers of *hnt*. The opposite direction of the genetic interaction in the eye *vs.* the embryo seen for *kst* and *chic* may reflect either differences in the role of *hnt* in regulating these proteins in distinct tissues or the different character of each of the *hnt* alleles (see discussion).

Genes that encode components of several signal transduction pathways genetically interact with *hnt*: We have previously shown that *basket* (which encodes JNK) and *dpp* (which encodes a TGFβ/BMP homolog and is a potential transcriptional target of JNK signaling) act as dominant suppressors of hnt^{308} (Reed *et al.* 2001). Furthermore, by assaying the intracellular localization of JUN and FOS, as well as *dpp* and *puc* transcription (*puc* encodes a JNK phosphatase and is also a transcriptional target of JNK signaling), we showed that HNT downregulates the JNK signaling pathway (Reed *et al.* 2001).

Here we detected dominant genetic interactions between hnt^{peb} and members of several signal transduction pathways (Table 2), including those mediated by JNK, TGFβ/BMP, Notch/Delta, and epidermal growth factor receptor (EGFR). Of particular interest in light of our previous results on JNK signaling, *tkv* mutations act as dominant suppressors of both the hnt^{peb} rough eye phenotype and hnt^{308} embryonic lethality (*tkv* encodes a DPP receptor; Figure 4; Tables 2 and 3) while puc^{A251} acts as a mild dominant suppressor of the hnt^{peb} eye phenotype and also shows mild, albeit not statistically significant, dominant suppression of hnt^{308} (Figure 4; Table 3). Three *Dl* alleles dominantly enhance the hnt^{peb} rough eye phenotype (Figure 1D; Table 2); one of these, Dl^{05151}, was tested in the embryo and significantly suppresses hnt^{308} embryonic lethality (Figure 4; Table 3).

There are several possible interpretations—not mutually exclusive—of the *hnt* genetic interactions with multiple signaling pathways. First, HNT may primarily regulate JNK signaling, with only indirect effects on, for example, the DPP/BMP pathway since this pathway is transcriptionally regulated in response to JNK. Second, HNT may independently regulate the production of components of the JNK, DPP/BMP, and Notch/Delta signaling pathways. Third, HNT may directly regulate production of proteins that are required for more than one cell-cell signaling pathway (*e.g.*, components of the extracellular matrix that regulate ligand binding).

Genes that encode components of the ECM genetically interact with *hnt*: The basal lamina, a specialized ECM, is composed mainly of collagen type IV and laminin. hnt^{peb} is dominantly suppressed by six different alleles of *viking* (collagen IV α2 chain) and two alleles of *Cg25C* (collagen IV α1 chain; Table 2). Five of the six tested alleles of *viking* and both of the *Cg25C* alleles also genetically interact with hnt^{308} (Table 3; Figure 4). Moreover, two *LanA* alleles ($LanA^{3A1}$ and $LanA^{4A8}$; LanA encodes laminin-α chain) suppress hnt^{308} embryonic lethality (Table 3; Figure 4). The direction of the genetic interactions among alleles of *viking* and hnt^{308} varies (Table 3; Figure 4): two alleles suppress embryonic lethality (vkg^{01209} and vkg^{177}), three are enhancers (vkg^{k16721}, vkg^{k00236}, and vkg^{k07138}), and one shows no significant genetic interaction (vkg^{k16502}). Some of the differences in the direction of the genetic interaction between specific *vkg* and *hnt* alleles may derive from the genetic complexity of the *vkg* locus (see Table 4 and discussion).

HNT controls the expression of genetically interacting genes both tissue autonomously and tissue nonautonomously: To establish which interacting genes might be directly regulated by HNT, we analyzed their expression in *hnt* mutants. Tests were carried out on a subset of interacting genes selected because they are expressed in at least two of three HNT-expressing tissues (amnioserosa, tracheal system, and/or the larval eye disc). To carry out the tests we used antibodies or enhancer trap lines where the *P* element is inserted in the gene of interest and there is detectable β-galactosidase reporter gene expression in the amnioserosa, the tracheal system, and/or the larval eye disc: *Dl*, *RhoA*, *puc*, *apontic*, and *dpp* could be examined in the embryo and *Dl*, *dpp*, *apontic*, and *kst* in the eye disc. *dpp* and *puc* served as a controls since they had already been shown to be downregulated by HNT in the amnioserosa and eye (Reed *et al.* 2001; Pickup *et al.* 2002). In the case of the developing eye disc, since the mutations assayed are embryonic lethals, patches of hnt^{XE81} or hnt^{EH704a} mutant tissue were generated using the FLP/FRT system (see materials and methods). The results of our analyses are pre-

TABLE 4

Complementation of *viking* alleles

	01209 S	*177-27* S	*k00236* E	*k07138* E	*k16502* NI
01209 S	−				
177-27 S	−[a]	−			
k00236 E	+[b]	−[a]	−		
k07138 E	−[b]	−[a]	−[a]	−	
k16502 NI	+[a,b]	−[a]	−[b]	−[a]	−

The first column and the first row show the genetic results obtained with hnt^{308} with different *vkg* alleles. S, suppressor; E, enhancer; NI, no interaction; −, fails to complement; +, complements. $vkg^{177\text{-}27}$ fails to complement the semilethal allele vkg^{k16721} (not shown).

[a] Lethal complementation tests done by us.

[b] Complementation tests reported by FlyBase (http://flybase.bio.indiana.edu).

sented in Figures 5 and 6 and are categorized by cellular process below.

Transcription (*apt*): During embryonic development *apontic* is expressed in the dorsal vessel, the tracheae, the amnioserosa, and the epidermal leading edge (Figure 5, A and C). In *hnt* mutant embryos the expression of *apontic* in the amnioserosa is not significantly altered (compare arrowheads in Figure 5, C *vs.* D) but leading edge expression is greatly reduced (compare open arrowhead in Figure 5, C *vs.* D). To visualize dorsal vessel and tracheal expression of *apontic*, which is not detectable using a single copy of the *apontic* enhancer trap, we used an APT-specific antibody. Wild-type embryos show APT expression in the dorsal vessel (arrowheads in Figure 5A), the embryonic tracheal system (open arrowhead in Figure 5A, brown staining), and the head (data not shown). In *hnt* mutant embryos all of these tissues show very reduced APT levels (Figure 5B). When HNT expression is removed specifically from tracheal cells using $Df(1)rb^{1}$ (Wilk *et al.* 2000), APT levels are reduced only in the tracheal system (data not shown). We conclude that HNT regulates *apontic* in both a tissue autonomous (tracheal cells) and a tissue nonautonomous (dorsal vessel, leading edge, and head) manner.

In the developing eye disc, APT protein is expressed in all peripodial membrane cells, as well as in the disc epithelium where APT is found in clusters of cells in the morphogenetic furrow, in the emerging R8 cell precursors, and then, more posteriorly, in basal undifferentiated disc cells (see wild-type tissue in Figure 6, B and C). In *hnt* mutant patches ($n = 10$) the peripodial membrane and basal epithelial staining is unaffected (data not shown), but APT expression in the early R8 precursor cell persists or is elevated for two to three additional, more posterior, rows compared to that in wild-type tissue (magenta arrowheads in Figure 6B). This effect is subtle but reproducible and suggests that HNT may be necessary tissue or cell autonomously for downregulation of *apontic* expression in the R8 precursor cell.

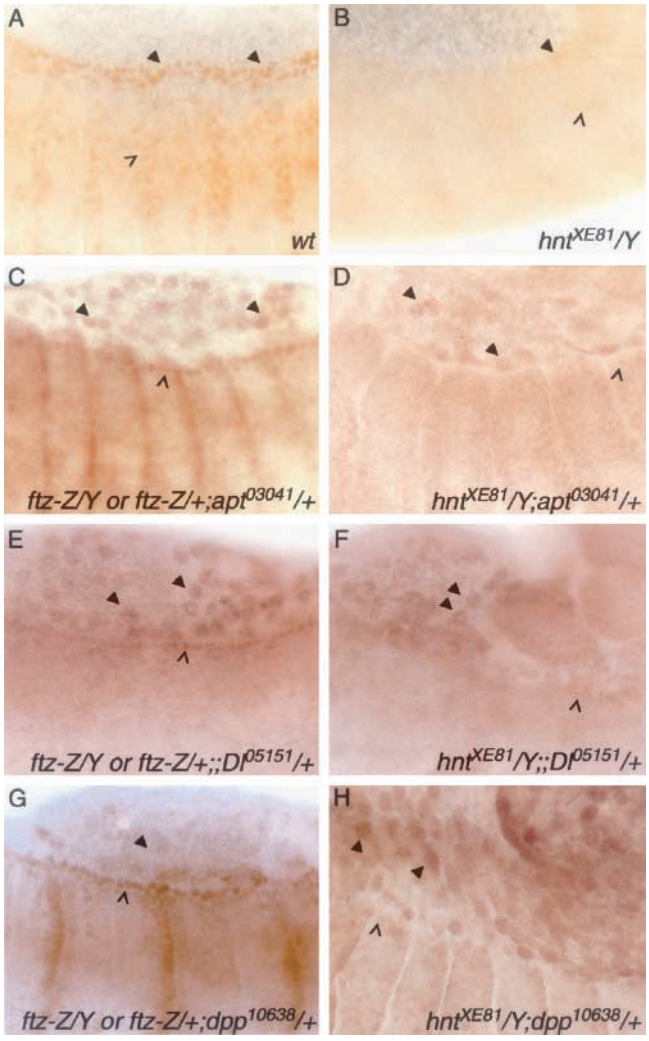

Figure 5.—HNT regulates candidate interacting genes tissue autonomously and nonautonomously in the embryo. (A and B) Wild-type (A) and hnt^{XE81} (B) stage 14 embryos showing APT protein in the dorsal vessel (arrowheads) and the tracheal system (open arrowhead). APT expression can be seen to be very reduced in the *hnt* mutant. (C–H) Expression reported by *lacZ* enhancer trap lines detected with anti-β-galactosidase antibody. The left column shows embryos with one copy each of the *lacZ* insertion and the *FM7, ftz-lacZ* balancer chromosome. The latter distinguishes these embryos from their hnt^{XE81} male siblings (right column). *apontic* (*apt*) expression in the leading edge (open arrowhead in C) is almost absent in *hnt* mutant embryos (open arrowhead in D), whereas the amnioserosal expression is not altered (arrowheads in C and D). A similar result is seen with *Delta* (*Dl*) expression (E *vs.* F; leading edge, open arrowheads; amnioserosa, arrowheads). *dpp* expression is upregulated in the amnioserosa of *hnt* mutant embryos (arrowheads in G *vs.* H) while epidermal leading edge expression is nonautonomously reduced (open arrowheads in G and H).

Signal transduction (*Dl*, *dpp*, and *puc*): In embryos, *Dl-lacZ* enhancer trap expression is found in the amnioserosa (arrowheads in Figure 5E), the leading edge (open arrowhead in Figure 5E), and the tracheal system (not detectable with a single copy of this *Dl* enhancer trap line). In

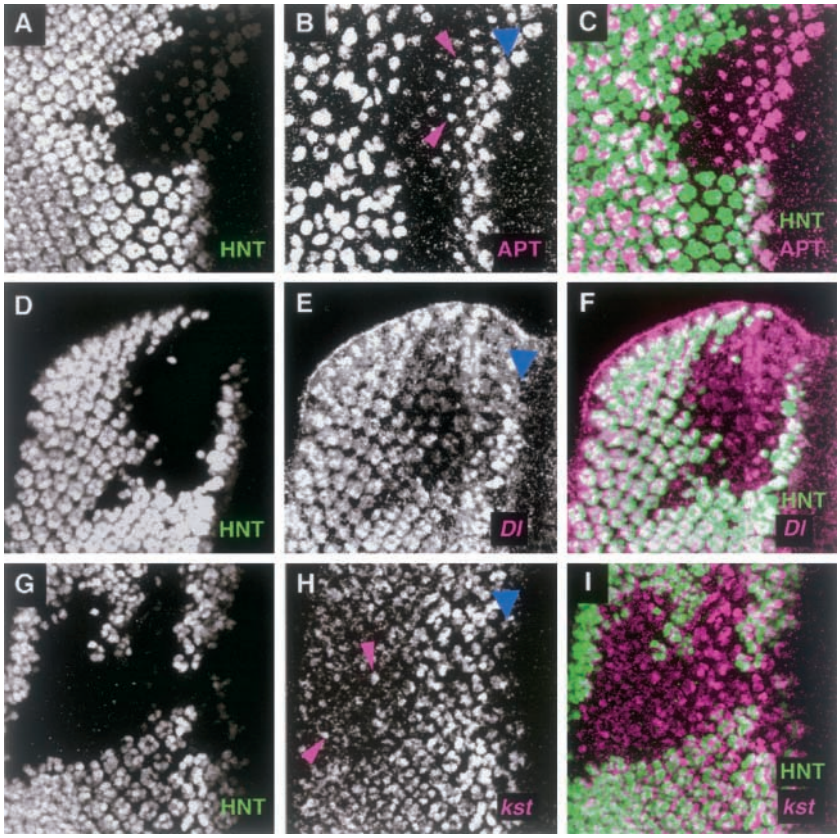

Figure 6.—HNT regulates candidate genes in the larval eye disc. (A–C) Confocal images of a third instar larval eye disc, which contains an hnt^{EH704a} mutant patch. The discs were double immunostained with anti-HNT (A) to visualize the patch and an anti-APT antibody (B). (C) The two single channels are merged. APT expression persists or is elevated in a single R cell for several rows just posterior to the furrow (magenta arrowheads) compared to the adjacent wild-type tissue. (D–F) Confocal images of an eye disc containing a clone of hnt^{XE81} tissue and marked with the Dl^{05151} enhancer trap line. The disc is double stained with anti-HNT antibody (D) and a chicken anti-β-galactosidase antibody (E), which reports *Dl-lacZ* expression. The two single channels are merged in F. Within the *hnt* patch, *Dl-lacZ* expression levels are reduced in all of the R cell precursors posterior to the furrow. (G–I) Confocal images of a disc with an hnt^{XE81} clone and marked with the kst^{03041} enhancer trap line. The disc is double stained with anti-HNT antibody (G) and a rabbit anti-β-galactosidase antibody (H), which reports the *kst-lacZ* expression. (I) The two single channels are merged. The initial *kst* expression looks unaffected in the *hnt* mutant tissue but by rows 10 and 11 the *kst* expression level is somewhat reduced and/or more diffuse in the R precursor cells than in the neighboring wild-type tissue. Occasionally a few apical cells are seen in this posterior region of the mutant tissue that have elevated *kst* expression (for examples see magenta arrowheads). Blue arrowheads mark the morphogenetic furrow in B, E, and H.

hnt mutant embryos, leading edge expression is greatly reduced (compare open arrowhead in Figure 5, E *vs.* F), while amnioserosal expression remains unchanged (compare arrowheads in Figure 5, E *vs.* F). Since HNT itself is not expressed in the leading edge, HNT must regulate *Dl* expression in the leading edge cells in a cell and tissue nonautonomous manner. In the third instar eye disc, *Dl-lacZ* enhancer trap expression is found in all of the R cell precursor cells posterior to the furrow (refer to wild-type tissue in Figure 6E). In hnt^{EH704a} mutant tissue ($n = 8$) *Dl-lacZ* expression is reduced in all of the R cells (Figure 6, E and F). This effect is seen specifically with the chicken anti-β-galactosidase antibody (ab-cam) and has been confirmed with X-GAL staining (data not shown). The same effect is not obvious with the rabbit anti-β-galactosidase antibody (Cappel) used in other experiments, suggesting that the reduction in *Dl-lacZ* expression is moderate and can be detected only at a certain threshold of staining.

HNT downregulates *dpp* and *puc* in the amnioserosa of hnt^{308} mutant embryos (Reed *et al.* 2001). Here we analyzed an amorphic *hnt* allele (hnt^{XE81}). In wild type, *dpp* and *puc* expression in the amnioserosa is very weak (for *dpp*, see Figure 5G, arrowhead; data not shown for *puc*) whereas, in hnt^{XE81} mutant embryos, *dpp* and *puc* expression in the amnioserosa is significantly elevated (for *dpp*, compare arrowheads in Figure 5, G *vs.* H), consistent with tissue autonomous downregulation of *dpp* and *puc* expression by HNT. Downregulation of *dpp* by HNT has been shown previously in *hnt* mutant eye tissue where the expression of a *dpp-lacZ* reporter is elevated in photoreceptor precursor cells posterior to the furrow (Pickup *et al.* 2002). In the embryo, HNT may have an additional, tissue nonautonomous, effect on *dpp* expression levels: *dpp* leading edge expression is clearly reduced in *hnt* mutant embryos (compare open arrowhead in Figure 5, G *vs.* H), suggesting that upregulation of *dpp* in the leading edge cells requires HNT function in the amnioserosa.

Cytoskeleton (*RhoA* and *kst*): Amnioserosal expression of *RhoA* is unchanged in *hnt* mutant embryos (data not shown) and was not assayed in the eye disc. In the eye disc, *kst-lacZ* expression is found in clusters of cells in the furrow and then in all of the emerging R cell precursors (see wild-type area of Figure 6H). In clones of hnt^{XE81} mutant tissue ($n = 7$) the early expression of *kst-lacZ* looks normal, but in more posterior regions of the clones (rows 10 and 11 and more posteriorly) the *kst-lacZ* staining declines or is absent in most cells when compared to the adjacent nonmutant tissue (Figure

6H). When we examined mosaic clusters along the borders of *hnt* mutant clones, we found examples of clusters with only a single hnt^+ cell. In 50% of these cases, this hnt^+ cell exhibited the same reduced level of *kst-lacZ* expression as its neighboring, mutant precursor cells, suggesting that the regulation of *kst* by HNT may have a cell nonautonomous component to it. This result is consistent with previous observations in which we showed that some of the mutant phenotypes in *hnt* mutant eye tissue are partially cell nonautonomous (Pickup *et al.* 2002). At this stage there are also a few dispersed R precursor cells (defined as such because the nuclei are apical and stain with anti-ELAV antibody; data not shown) that have higher than wild-type levels of *kst-lacZ* staining (Figure 6H, magenta arrowheads).

In summary, we have identified five genes whose expression levels are regulated tissue autonomously by HNT (*apt*, *Dl*, *dpp*, *kst*, and *puc*). Three of these (*apt*, *Dl*, and *dpp*) are also regulated tissue nonautonomously by HNT.

Collagen IV and laminin deposition and/or maintenance in the basal lamina of the developing tracheal system are affected in *hnt* mutant embryos: In Drosophila, procollagen IV (Lunstrum *et al.* 1988) and laminin-α (Kusche-Gullberg *et al.* 1992) are synthesized in the circulating blood cells, which are known as hemocytes. Subsequently, collagen IV and laminin are deposited in the basement membranes of major organs (Fessler and Fessler 1989; Montell and Goodman 1989; Yarnitzky and Volk 1995; Martin *et al.* 1999). Since HNT is not expressed in any mesodermal derivatives, including the hemocytes, any effects on collagen IV and laminin distribution in HNT-expressing tissues must derive from HNT-dependent defects in processing, deposition, or maintenance of these molecules in the basal lamina of that tissue. The basal lamina plays a pivotal role in maintenance of tissue integrity (reviewed by Yurchenco and O'Rear 1994; Ashkenas *et al.* 1996; Wilk *et al.* 2004). Our previous studies of the role of HNT during tracheal development clearly showed that HNT regulates tracheal tissue integrity (Wilk *et al.* 2000). Because the embryonic tracheal system has a defined basal lamina (Tepass and Hartenstein 1994) and mutations in collagen IV and laminin exhibit particularly strong dominant genetic interactions with *hnt*, we chose to analyze collagen IV and laminin deposition during embryonic tracheal development in wild-type and *hnt* mutant embryos utilizing specific antibodies and tracheal markers (see materials and methods).

Collagen IV is present at high levels in hemocytes (asterisks in Figure 7A), the fat body (not shown), and basement membranes (arrowheads in Figure 7, A and A′; see also Fessler and Fessler 1989). As the tracheae develop, collagen IV (stage 14 onward) and laminin (stage 13 onward) can be detected on the basal side of the tracheal cells (Figure 7, A, A′, and D; arrowheads, stage 15 embryos). To determine whether basal collagen IV and laminin deposition are affected in the tracheae of *hnt* mutant embryos, we analyzed the tracheal tissue of two amorphic *hnt* alleles (hnt^{XE81} and hnt^{1142}; identical results were obtained for both alleles). As expected, *hnt* mutant embryos show normal levels of collagen IV in hemocytes (Figure 7, C and C′; asterisks). Basal localization of collagen IV in the developing tracheal epithelia occurs in *hnt* mutants (Figure 7, B′ and C′). However, *hnt* mutant tracheae show a patchy and discontinuous collagen IV distribution when compared to wild-type tracheae. By late embryonic stage 14, this phenotype is more pronounced: each embryo has areas with marked reductions or complete absences of collagen IV (Figure 7, B and B′; open arrowhead and arrows, respectively) as well as patches of overaccumulation (Figure 7, C and C′; solid arrowheads). Tracheal laminin distribution at stage 13 is identical in *hnt* and wild-type embryos (data not shown). As for collagen, by stage 14, *hnt* embryos have patchy or discontinuous laminin staining in the basal lamina of their tracheae compared to wild type (arrowhead in Figure 7D *vs.* arrowhead in Figure 7E).

We conclude that, while *hnt* does not directly regulate the expression of either collagen IV or laminin, it is required in HNT-expressing tissues, such as the trachea, for collagen IV and laminin deposition, distribution, or maintenance in the basal lamina.

DISCUSSION

Here we have identified >60 loci that exhibit dose-sensitive genetic interactions with hnt^{peb}, a viable rough-eyed *hnt* allele, and have shown that the majority of a subset of these that were tested for interaction with hnt^{308} also modify the embryonic lethality associated with that allele. The direction of the dominant genetic interactions is not always the same in the eye and embryo. We do not believe that this difference is due to a difference in the nature of the two *hnt* alleles since both behave as hypomorphs (Yip *et al.* 1997; Reed *et al.* 2001; Pickup *et al.* 2002): hnt^{308} is caused by a *P*-element insertion 509 nucleotides upstream of the transcription start site and results in reduced accumulation of HNT protein, particularly in the amnioserosa (Reed *et al.* 2001). hnt^{peb} shows defects only in eye development, and HNT expression levels are normal in hnt^{peb} mutant eyes. We therefore presume that hnt^{peb} is caused by a point mutation that alters the function rather than the expression level or pattern of HNT protein (we have not yet been able to detect any sequence alterations in the open reading frame; A. T. Pickup and H. D. Lipshitz, unpublished observations).

An alternative hypothesis is that the role of *hnt* in regulating the cellular process affected by the interactor may differ in the eye and the embryo. Differences in direction of interaction occur for *Dl* (enhancer of eye phenotype, suppressor of embryonic lethality), *chic* (suppressor of eye phenotype, enhancer of embryonic lethality), and *kst* (suppressor of eye phenotype, en-

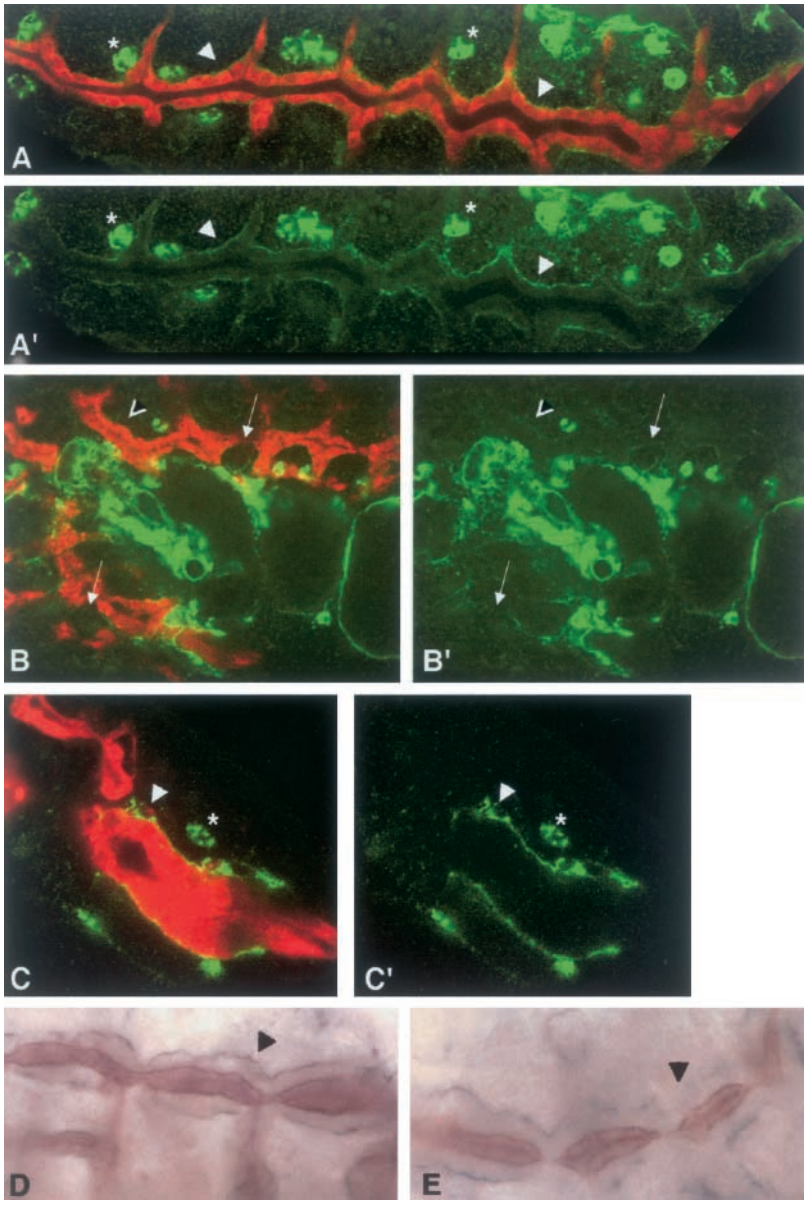

FIGURE 7.—Collagen type IV and laminin are abnormally distributed in the basal lamina of *hnt* mutant tracheae. Confocal images from either *+/+;1-eve-1* (A) or *hnt;1-eve-1* mutant embryos (B and C) that were double stained for a tracheal cell marker, shown in red (see MATERIALS AND METHODS), and with mouse monoclonal anti-collagen IV antibody, shown in green. Primes show the green channel only (only the collagen IV staining). Collagen IV expression can be seen in the hemocytes (asterisks) and in the basal lamina of the tracheal system (arrowheads). The distribution of collagen IV is less uniform in *hnt* mutant tracheae than in wild type: absent (arrows in B), weaker (open arrowhead in B), or stronger and patchy (arrowhead in C). Light microscope images from wild-type (D) or *hnt* (E) embryos immunostained for laminin (purple) and tracheal lumen antibody 55 (brown). Arrowheads show laminin staining in the basal lamina of the developing tracheae, evenly distributed in wild type (D) but uneven and patchy in *hnt* mutant embryos (E).

hancer of embryonic lethality). The fact that the direction of interaction changes in the same way for both cytoskeletal regulatory proteins (*chic* and *kst*), which function to regulate F actin assembly, is consistent with this alternative hypothesis. However, since the exact cause of embryonic lethality in hnt^{308} is unknown (REED *et al.* 2001) and the hnt^{peb} eye phenotype is complex (PICKUP *et al.* 2002), understanding the reason for the particular direction of any specific genetic interaction is likely to come only with a more detailed understanding of the molecular pathways regulated by HNT and the particular role of HNT in transcriptional control. In regard to the latter, for example, it will be important to assess whether different HNT cofactors might be present in different tissues.

In the case of *vkg* (which encodes collagen IV), the direction of the genetic interaction with *hnt* differs for different *vkg* alleles. For example, all six *vkg* alleles are suppressors of hnt^{peb}; however, two of the five alleles that interact with hnt^{308} are suppressors and three are enhancers. Thus, the direction of interaction differs not only for the two *hnt* alleles, but also for different *vkg* alleles. It is likely that this additional layer of complexity derives from the fact that *vkg* alleles themselves show complex interallelic complementation (Table 4; see also GELLON *et al.* 1997), possibly because collagen forms multimers (of two α1 chains and one α2 chain) in the extracellular matrix.

We have previously shown that the HNT zinc-finger protein is expressed in specific tissues in each of which it regulates cell differentiation, epithelial integrity, and cell survival (YIP *et al.* 1997; LAMKA and LIPSHITZ 1999; WILK *et al.* 2000; REED *et al.* 2001; PICKUP *et al.* 2002). During at least two morphogenetic processes—embryonic

dorsal closure and retinal differentiation—we have reported defects in the F actin-based cytoskeleton in *hnt* mutants. In the embryo, these defects are tissue nonautonomous, since they occur in the leading edge cells that are not themselves expressing HNT but are closely apposed to HNT-expressing amnioserosal cells (Reed *et al.* 2001). In the eye, the defects may be cell autonomous, occurring in the photoreceptor cells, each of which expresses HNT (Pickup *et al.* 2002). In addition to these cytoskeletal defects, we have presented evidence that HNT downregulates JNK signaling in both the amnioserosa and, possibly, the eye (Reed *et al.* 2001; Pickup *et al.* 2002). Finally, HNT is required in the amnioserosa, tracheal system, and eye disc to maintain epithelial integrity; in *hnt* mutants, these tissues fall apart and the cells subsequently undergo apoptosis (Frank and Rushlow 1996; Lamka and Lipshitz 1999; Wilk *et al.* 2000; Pickup *et al.* 2002; Reed *et al.* 2004).

Since HNT is a nuclear Zn-finger protein with all of the hallmarks of a transcription factor, the cellular and tissue phenotypes seen in *hnt* mutants are likely to be an indirect consequence of defects in transcriptional control. However, the particular molecular pathway(s) affected in *hnt* mutants are unknown. Our screen for dominant genetic interactors with *hnt* mutants was thus motivated in large part by the desire to identify potential genetic pathways that are regulated, directly or indirectly, by HNT. Because the screen initially focused on modification of the hnt^{peb} rough eye phenotype and then retested the interactors for modification of the hnt^{308} embryonic lethal phenotype, both eye-specific and general modifier genes could be identified. Our initial focus was primarily on loci that act as dominant modifiers of both phenotypes and are expressed in the same tissues as HNT and thus are candidates for HNT regulation—directly or indirectly—in all tissues in which it is expressed. In this regard, it is clear that mutations in several types of genes modify the *hnt* phenotype: these include genes that encode other transcription factors (*e.g.*, *apt*), signal transduction molecules (*e.g.*, *Dl*, and *dpp*), and regulators of the actin-based cytoskeleton (*e.g.*, *chic*, *RhoA*, and *kst*).

Our assays of effects on expression of a subset of these interactors allowed us to identify which might be direct targets of HNT transcriptional control and which are unlikely to fall into this category. Candidates for direct regulation by HNT include *apt*, *Dl*, *dpp*, *kst*, and *puc* since their expression is altered in a tissue autonomous way in *hnt* mutants. In the cases of *dpp* and *puc*, the role of HNT appears to be to downregulate their expression, while HNT's role is to upregulate *Dl* and *kst* expression. For *apt*, HNT functions either to downregulate (in the eye) or to upregulate (in the tracheae) expression. It has recently been reported that the mammalian homolog of HNT, RREB-1/Finb, can function as a DNA-binding protein that acts to "potentiate" transcriptional activation by the BETA2/NeuroD basic helix-loop-helix protein (Ray *et al.* 2003). Whether HNT acts as a transcriptional potentiator and, additionally, as a DNA-binding "antipotentiator," remains to be determined. Of interest in this regard is the fact that the effects on candidate target gene expression that we have seen in the eye disc appear to involve a reduction or increase in levels, not an absolute on/off control.

Two of the candidate HNT target genes, *dpp* and *puc*, are transcriptional targets of JNK signaling, presumably of the AP-1 transcription factor (Glise and Noselli 1997; Hou *et al.* 1997; Riesgo-Escovar and Hafen 1997a,b; Sluss and Davis 1997; Zeitlinger *et al.* 1997). This raises the interesting possibility that one of HNT's roles may be to regulate AP-1 activity. For example, HNT might prevent AP-1 from activating some or all of its target genes by competing for AP-1 binding sites, by binding to AP-1 components and preventing them from binding to DNA, or by binding to the same target genes but functioning as a repressor.

Another *hnt*-interactor, *chic* (which encodes profilin, Cooley *et al.* 1992), plays a role in embryonic dorsal closure and larval eye morphogenesis (Jasper *et al.* 2001; Benlali *et al.* 2002), two processes in which HNT functions. Furthermore, the *chic* gene has been identified as a JNK pathway target gene in a screen that used serial analysis of gene expression (Jasper *et al.* 2001). It is therefore possible that defects in AP-1 target gene regulation in *hnt* mutants may underlie the genetic interaction between *hnt* and *chic* reported here. An alternative is that the genetic interaction results from nonautonomous effects of *hnt* mutants on the leading edge of the epidermis (Reed *et al.* 2001). *chic* mutants show defects in leading edge filopodia during dorsal closure (Jasper *et al.* 2001). It is thus possible that *chic* mutants enhance the embryonic lethality of hnt^{308} by further increasing the disruption of actin-rich structures at the leading edge that is caused nonautonomously by *hnt* mutant amnioserosal tissue.

Several interactors are regulated both tissue autonomously and tissue nonautonomously by *hnt*. For example, HNT tissue autonomously regulates *apt*, *dpp*, *kst*, and *Dl* in the developing retina; *apt* in the tracheae; and *dpp* in the amnioserosa. However, in *hnt* mutants but not in wild type, *apt*, *Dl*, and *dpp* expression is absent from the epidermal leading edge cells. Similarly, *apt* is expressed in the dorsal vessel in wild type but not in *hnt* mutants. Since HNT is not expressed in leading edge cells or the dorsal vessel, these effects must be tissue nonautonomous. We have previously presented extensive evidence that HNT-dependent downregulation of JNK signaling in the amnioserosa is required for assembly of the F actin-based purse string in the epidermal leading edge and have hypothesized that this occurs only at a high-low JNK signaling boundary (Reed *et al.* 2001). It is therefore possible that HNT-dependent upregulation of genes such as *apt*, *Dl*, and *dpp* in the leading edge also requires such a boundary. A recent screen for car-

diogenic genes has reported a requirement for *hnt* in assembly of the heart tube and for heart patterning (Kim *et al.* 2004). Since dorsal closure is required for assembly of the heart but fails in *hnt* mutants, some of the cardiogenic defects in *hnt* mutants may derive indirectly from the dorsal closure defect. However, the absence of *apt* expression in the dorsal vessel of *hnt* mutants that we have observed here may underlie specific heart pattern defects observed in that study.

In light of the previously reported tissue integrity defects in *hnt* mutants (Lamka and Lipshitz 1999; Wilk *et al.* 2000; Pickup *et al.* 2002), we were particularly interested in the strong genetic interactions between *hnt* and components of the extracellular matrix (collagen IV subunits and laminin). The most detailed analyses of these defects had been carried out in the embryonic tracheal system, where we previously showed that *hnt* mutant tracheal cells have normal crumbs and DE-cadherin distribution, adherens junctions, and apical-basal polarity (Wilk *et al.* 2000); however, in that study, the basal lamina was not investigated. Given the strong genetic interactions between *hnt* and genes encoding components of the basal lamina, together with the known role of the basal lamina in maintenance of epithelial integrity, we focused here on the distribution of collagen IV and laminin in the basal lamina of *hnt* mutant tracheae. We have shown that deposition or maintenance of collagen IV and laminin is abnormal in the basal lamina of *hnt* mutant tracheae, although we cannot at present definitively determine whether this is the cause of the loss of integrity. Interestingly, when collagen IV levels are reduced during Drosophila embryogenesis, transgenic embryos show defects in germ band retraction and dorsal closure (Borchiellini *et al.* 1996), two processes for which HNT is essential (Yip *et al.* 1997; Lamka and Lipshitz 1999; Reed *et al.* 2001). Moreover, *LanA* embryos have defects in the tracheal dorsal trunk that are similar those described for *hnt* mutant embryos (Stark *et al.* 1997; Wilk *et al.* 2000). The less severe defect in the *LanA* mutants than in *hnt* may reflect the fact that, even without laminin, collagen IV can still assemble a meshwork in basal epithelia (both alleles used here are amorphic, see Henchcliffe *et al.* 1993; Yarnitzky and Volk 1995).

Since both collagen and laminin are synthesized primarily in the circulating hemocytes, which deposit these molecules in the basal lamina during its construction, and HNT is not expressed in the hemocytes, the defects in deposition of these basal lamina components in *hnt* mutants must be indirect. We have recently demonstrated that integrin-dependent membrane interactions between the yolk sac membrane and the amnioserosa are essential for amnioserosal epithelial integrity and to prevent anoikis (Reed *et al.* 2004). We hypothesized that membrane apposition may be abnormal in *hnt* mutants, leading to premature anoikis. Since it is known that laminin-integrin physical interaction plays a key role in assembly of the basal lamina (reviewed in Wilk *et al.* 2004), it will be of interest to determine whether integrin expression is normal in HNT-expressing epithelia. Defects in integrin expression in *hnt* mutant epithelia may underlie abnormalities in the basal lamina and genetic interactions with extracellular membrane proteins, as well as many of the other genetic interactions we have reported here (*e.g.*, with signal transduction pathway and cytsokeletal components). Alternatively, since it is known that the ECM plays a key role in signal transduction (reviewed by Gumbiner 1996; Lauffenburger and Horwitz 1996; Wilk *et al.* 2004), the phenotypic effects of HNT may be indirect via regulation of ECM deposition and maintenance. In βPS and αPS3 integrin mutants, germ band retraction and dorsal closure fail and there are defects in tracheal development (Wieschaus and Noell 1986; Leptin *et al.* 1989; Bunch *et al.* 1992; Stark *et al.* 1997). The similarity of the integrin and *hnt* mutant phenotypes is thus consistent with the possibility that integrin expression or function is regulated by HNT.

We thank the Bloomington Drosophila Stock Center for hundreds of the stocks provided for this study. Thanks also go to J. Duffy, S. L. Zipursky, N. McGinnis, B. Shilo, M. Krasnow, L. I. Fessler, U. Tepass, and R. Schuh for providing fly stocks and reagents. R.W. was supported in part by an Ontario Graduate Scholarship and a studentship from the Ontario Student Opportunity Trust Fund-Hospital for Sick Children Foundation Student Scholarship Program; A.T.P. was supported in part by a postdoctoral fellowship from the Hospital for Sick Children Research Training Centre; J.K.H. was supported in part by an Eli Lilly Canada-Medical Research Council/Pharmaceutical Manufacturer's Association of Canada Health Program Fellowship. H.D.L. is Canada Research Chair (CRC, Tier 1) in Developmental Biology at the University of Toronto. This research was supported by funds from the CRC Program and an operating grant to H.D.L. from the National Cancer Institute of Canada with funds from the Canadian Cancer Society.

LITERATURE CITED

Ashkenas, J., J. Muschler and M. J. Bissell, 1996 The extracellular matrix in epithelial biology: shared molecules and common themes in distant phyla. Dev. Biol. **180:** 433–444.

Benlali, A., I. Draskovic, D. Hazelett and J. Treisman, 2002 act up controls actin polymerization to alter cell shape and restrict Hedgehog signaling in the Drosophila eye disc. Cell **101:** 271–281.

Borchiellini, C., J. Coulon and Y. Le Parco, 1996 The function of type IV collagen during Drosophila muscle development. Mech. Dev. **58:** 179–191.

Bunch, T. A., R. Salatino, M. C. Engelsgjerd, L. Mukai, R. F. West *et al.*, 1992 Characterization of mutant alleles of myospheroid, the gene encoding the beta subunit of the Drosophila PS integrins. Genetics **132:** 519–528.

Cooley, L., E. Verheyen and K. Ayers, 1992 chickadee encodes a profilin required for intercellular cytoplasm transport during Drosophila oogenesis. Cell **69:** 173–184.

Dixon, W. J., and F. J. Massey, Jr., 1957 *Introduction to Statistical Analysis.* McGraw-Hill, New York.

Eulenberg, K. G., and R. Schuh, 1997 The *tracheae defective* gene encodes a bZIP protein that controls tracheal cell movement during Drosophila embryogenesis. EMBO J. **16:** 7156–7165.

Fessler, J. H., and L. I. Fessler, 1989 Drosophila extracellular matrix. Annu. Rev. Cell Biol. **5:** 309–339.

Fessler, L. I., A. G. Campbell, K. G. Duncan and J. H. Fessler, 1987 Drosophila laminin: characterization and localization. J. Cell Biol. **105:** 2383–2391.

Frank, L. H., and C. Rushlow, 1996 A group of genes required for maintenance of the amnioserosa tissue in Drosophila. Development **122:** 1343–1352.

Geiger, B., A. Bershadsky, R. Pankov and K. M. Yamada, 2001 Transmembrane crosstalk between the extracellular matrix-cytoskeleton crosstalk. Nat. Rev. Mol. Cell. Biol. **2:** 793–805.

Gellon, G., K. W. Harding, N. McGinnis, M. M. Martin and W. McGinnis, 1997 A genetic screen for modifiers of Deformed homeotic function identifies novel genes required for head development. Dev. Suppl. **124:** 3321–3331.

Glise, B., and S. Noselli, 1997 Coupling of Jun amino-terminal kinase and Decapentaplegic signaling pathways in Drosophila morphogenesis. Genes Dev. **11:** 1738–1747.

Gumbiner, B. M., 1996 Cell adhesion: the molecular basis of tissue architecture and morphogenesis. Cell **84:** 345–357.

Henchcliffe, C., L. Garcia-Alonso, J. Tang and C. S. Goodman, 1993 Genetic analysis of laminin A reveals diverse functions during morphogenesis in Drosophila. Development **118:** 325–337.

Hou, X. S., E. S. Goldstein and N. Perrimon, 1997 Drosophila Jun relays the Jun amino-terminal kinase signal transduction pathway to the Decapentaplegic signal transduction pathway in regulating epithelial cell sheet movement. Genes Dev. **11:** 1728–1737.

Jasper, H., V. Benes, C. Schwager, S. Sauer, S. Clauder-Munster *et al.*, 2001 The genomic response of the Drosophila embryo to JNK singnaling. Dev. Cell **1:** 579–586.

Kim, Y.-O., S.-J. Park, R. S. Balaban, M. Nirenberg and Y. Kim, 2004 A functional genomic screen for cardiogenic genes using RNA interference in developing Drosophila embryos. Proc. Natl. Acad. Sci. USA **101:** 159–164.

Kusche-Gullberg, M., K. Garrison, A. J. MacKrell, L. I. Fessler and J. H. Fessler, 1992 Laminin A chain: expression during Drosophila development and genomic sequence. EMBO J. **11:** 4519–4527.

Lamka, M. L., and H. D. Lipshitz, 1999 Role of the amnioserosa in germ band retraction of the *Drosophila melanogaster* embryo. Dev. Biol. **214:** 102–112.

Lauffenburger, D. A., and A. F. Horwitz, 1996 Cell migration: a physically integrated molecular process. Cell **84:** 359–369.

Leptin, M., T. Bogaert, R. Lehmann and M. Wilcox, 1989 The function of PS integrins during Drosophila embryogenesis. Cell **56:** 401–408.

Lunstrum, G. P., H.-P. Barchinger, L. I. Fessler, K. G. Duncan, R. E. Nelson *et al.*, 1988 Drosophila basement membrane procollagen IV. J. Biol. Chem. **263:** 18318–18327.

Martin, D., S. Zusman, X. Li, E. L. Williams, N. Khare *et al.*, 1999 wing blister, a new Drosophila laminin α chain required for cell adhesion and migration during embryonic and imaginal development. J. Cell Biol. **145:** 191–201.

Montell, D. J., and C. S. Goodman, 1989 *Drosophila* Laminin: sequence of B2 subunit and expression of all three subunits during embryogenesis. J. Cell Biol. **109:** 2441–2453.

Pickup, T. A., M. L. Lamka, Q. Sun, M. L. R. Yip and H. D. Lipshitz, 2002 Control of photoreceptor cell morphology, planar polarity and epithelial integrity during Drosophila development. Development **129:** 2247–2258.

Ray, S. K., J. Nishitani, M. W. Petry, M. Y. Fessing and A. B. Leiter, 2003 Novel transcriptional potentiation of BETA2/NeuroD on the secretin gene promoter by the DNA-binding protein Finb/RREB-1. Mol. Cell. Biol. **23:** 259–271.

Reed, B. H., 1992 The genetic analysis of endoreduplication in Drosophila melanogaster, Ph.D. Thesis, University of Cambridge, Cambridge, UK.

Reed, B. H., R. Wilk and H. D. Lipshitz, 2001 Downregulation of Jun kinase signaling in the amnioserosa is essential for dorsal closure of the Drosophila embryo. Curr. Biol. **11:** 1098–1108.

Reed, B. H., R. Wilk, F. Schock and H. D. Lipshitz, 2004 Integrin-dependent apposition of Drosophila extraembryonic membranes promotes morphogenesis and prevents anoikis. Curr. Biol. **14:** 372–380.

Reichman-Fried, M., B. Dickson, E. Hafen and B.-Z. Shilo, 1994 Elucidation of the role of *breathless*, a *Drosophila* FGF receptor homolog, in tracheal cell migration. Genes Dev. **8:** 428–439.

Riesgo-Escovar, J. R., and E. Hafen, 1997a Common and distinct roles of DFos and DJun during Drosophila development. Science **278:** 669–672.

Riesgo-Escovar, J. R., and E. Hafen, 1997b Drosophila Jun kinase regulates expression of decapentaplegic via the ETS-domain protein Aop and the AP-1 transcription factor DJun during dorsal closure. Genes Dev. **11:** 1717–1727.

Sluss, H. K., and R. J. Davis, 1997 Embryonic morphogenesis signaling pathway mediated by JNK targets the transcription factor JUN and the TGF-beta homologue decapentaplegic. J. Cell. Biochem. **67:** 1–12.

Stark, K. A., G. H. Yee, C. E. Roote, E. L. Williams, S. Zusman *et al.*, 1997 A novel α integrin subunit associates with βPS and functions in tissue morphogenesis and movement during Drosophila development. Dev. Suppl. **124:** 4583–4594.

Tepass, U., and V. Hartenstein, 1994 The development of cellular junctions in the Drosophila embryo. Dev. Biol. **161:** 563–596.

Tepass, U., G. Tanentzapf, R. Ward and R. Fehon, 2001 Epithelial cell polarity and cell junctions in Drosophila. Annu. Rev. Genet. **35:** 747–784.

Thomas, G. H., and D. P. Kiehart, 1994 β_{Heavy}-spectrin has a restricted tissue and subcellular distribution during Drosophila embryogenesis. Development **120:** 2039–2050.

Van Aelst, L., and M. Symons, 2002 Role of Rho family GTPases in epithelial morphogenesis. Genes Dev. **16:** 1032–1054.

Verheyen, E. M., and L. Cooley, 1994 Profilin mutations disrupt multiple actin-dependent processes during Drosophila development. Dev. Suppl. **120:** 717–728.

Wieschaus, E., and E. Noell, 1986 Specificity of embryonic lethal mutations in *Drosophila* analyzed in germ line clones. Roux's Arch. Dev. Biol. **195:** 63–73.

Wilk, R., I. Weizman and B.-Z. Shilo, 1996 trachealess encodes a bHLH-PAS protein that is an inducer of tracheal cell fates in Drosophila. Genes Dev. **10:** 93–102.

Wilk, R., B. H. Reed, U. Tepass and H. D. Lipshitz, 2000 The hindsight gene is required for epithelial maintenance and differentiation of the tracheal system in Drosophila. Dev. Biol. **219:** 183–196.

Wilk, R., A. T. Pickup and H. D. Lipshitz, 2004 Epithelial morphogenesis, pp. 277–304 in *Encyclopedia of Molecular Cell Biology and Molecular Medicine*, edited by R. A. Meyers. Wiley-VCH, Weinheim, Germany.

Xu, T., and G. M. Rubin, 1993 Analysis of genetic mosaics in developing and adult *Drosophila* tissues. Development **117:** 1223–1237.

Yarnitzky, T., and T. Volk, 1995 Laminin is required for heart, somatic muscles, and gut development in the Drosophila embryo. Dev. Biol. **169:** 609–618.

Yip, M. L. R., M. L. Lamka and H. D. Lipshitz, 1997 Control of germ-band retraction in Drosophila by the zinc-finger protein HINDSIGHT. Development **124:** 2129–2141.

Yurchenco, P. D., and J. J. O'Rear, 1994 Basal lamina assembly. Curr. Opin. Cell Biol. **6:** 674–681.

Zeitlinger, J., L. Kockel, F. A. Peverali, D. B. Jackson, M. Mlodzik *et al.*, 1997 Defective dorsal closure and loss of epidermal decapentaplegic expression in Drosophila fos mutants. EMBO J. **16:** 7393–7401.

Communicating editor: T. Schüpbach